# MUSCARINIC RESPONSES OF RAT BASOLATERAL AMYGDALOID NEURONS RECORDED *IN VITRO*

## BY MARK S. WASHBURN* AND HYLAN C. MOISES

*From the Department of Physiology and Neuroscience Program, The University of Michigan, Ann Arbor, MI 48109-0622, USA*

### SUMMARY

1. Intracellular recordings were obtained from pyramidal-type neurons in the basolateral amygdaloid nucleus (BLA) in slices of rat ventral forebrain and used to compare the actions of exogenously applied cholinomimetics to the effects produced by electrical stimulation of amygdalopetal cholinergic afferents from basal forebrain.

2. Bath application of carbachol depolarized pyramidal cells with an associated increase in input resistance ($R_i$), reduced the slow after-hyperpolarization (AHP) that followed a series of current-evoked action potentials and blocked spike frequency accommodation. All of these effects were reversed by the muscarinic antagonist atropine but not by the nicotinic antagonist hexamethonium.

3. Electrical stimulation of amygdaloid afferents within the external capsule evoked a series of synaptic potentials consisting of a non-cholinergic fast excitatory postsynaptic potential (EPSP), followed by early and late inhibitory postsynaptic potentials (IPSPs). Each of these synaptic potentials was reduced by carbachol in an atropine-sensitive manner.

4. Local application of carbachol to pyramidal cells produced a short-latency hyperpolarization followed by a prolonged depolarization. The hyperpolarization and depolarization to carbachol were blocked by atropine but not hexamethonium.

5. The carbachol-induced hyperpolarization was associated with a decrease in $R_i$ and had a reversal potential nearly identical to that of the early IPSP. The inhibitory response was blocked by perfusion of medium containing tetrodotoxin (TTX), bicuculline or picrotoxin, while the subsequent depolarization was unaffected. On the basis of these data, it is concluded that the muscarinic hyperpolarization is mediated through the rapid excitation of presynaptic GABAergic interneurons in the slice.

6. The findings that the carbachol-induced depolarization was associated with an increase in $R_i$, often had a reversal potential below $-80$ mV, was sensitive to changes in extracellular potassium concentration and was blocked by intracellular iono-phoresis of the potassium channel blocker caesium suggest that it resulted from a muscarinic blockade of one or more potassium conductances.

7. Repetitive stimulation of sites within the slice containing cholinergic afferents

* Present address: Department of Neuroscience Pharmacology, Parke-Davis Research Division, Warner-Lambert Company, Ann Arbor, MI, 48105, USA.

evoked a series of fast EPSPs followed by IPSPs. These non-cholinergic potentials were followed by a slow EPSP that lasted from 10 s–4 min. The slow EPSP was enhanced by eserine and blocked by atropine. It was also blocked by TTX or cadmium, indicating that it was dependent on spike propagation and calcium-dependent release of acetylcholine (ACh).

8. Stimulation of cholinergic afferents in the slice mimicked other effects produced by carbachol including blockade of the slow AHP and accommodation of action potential discharge and these actions were potentiated by eserine and blocked by atropine.

9. The present results provide the first demonstration of muscarinic cholinergic actions in an area of the amygdala known to receive cholinergic innervation. These effects appear to involve both direct and indirect mechanisms.

### INTRODUCTION

Numerous studies using conventional acetylcholinesterase (AChE) histochemical techniques (Ben-Ari, Zigmond, Shute & Lewis, 1977; Emson, Paxinos, Le Gal La Salle, Ben-Ari & Silver, 1979; Nagai, Kimura, Maeda, McGeer, Peng & McGeer, 1982; Woolf & Butcher, 1982) or immunohistochemical staining for choline-acetyltransferase (ChAT) (Mesulam, Mufson, Levey & Wainer, 1983; Carlsen, Zaborskey & Heimer, 1985; Hellendall, Godfrey, Ross, Armstrong & Price, 1986) have demonstrated that the amygdaloid complex in the rat receives a very dense cholinergic innervation from regions of the basal forebrain. Results from these studies and recent investigations involving quantitative microassay for ChAT (Hellendall *et al.* 1986) have revealed that the nuclei contained within the basolateral amygdaloid complex serve as the major targets of this basal forebrain cholinergic input. The basolateral nucleus (BLA), in particular, displays the highest content of cholinergic enzymatic markers with lesser amounts found in the lateral and basomedial nuclei (Ben-Ari *et al.* 1977; Hellendall *et al.* 1986). Immunohistochemical analyses for ChAT indicate that cholinergic input to cells in the BLA is derived largely from extrinisic afferents that originate from cholinergic neurons located in the substantia inominata, while a lesser component of this cholinergic innervation is derived from a dispersed continuum of cells that stretches from the nucleus of the diagonal band of Broca through the ventral pallidum and along the ansa lenticularis (Emson *et al.* 1979; Woolf & Butcher, 1982; Carlsen *et al.* 1985). While the vast majority of the cholinergic innervation of rat BLA arises from extrinsic sources, Carlsen & Heimer (1986) have identified a small population of intrinsic cholinergic neurons in this nucleus, which according to their measurements constitute less than 5% of the total complement of constituent cells.

Despite the wealth of anatomical data regarding the cholinergic innervation of the BLA, little is known about the role this projection might play in regulating amygdaloid neuronal activity. This situation in part reflects the relative paucity of basic information that is available concerning the cellular physiology of constituent neuronal elements in this brain region. Recent anatomical work has stressed the close functional relationship between the BLA and brain areas, such as hippocampus and cortex, and has drawn attention to the similarity between their intrinsic organizational features (Carlsen & Heimer, 1988). It therefore seemed a reasonable

question to ask whether acetylcholine (ACh) and cholinomimetics have actions in BLA similar to those found in hippocampus and cortex, each of which also receives a prominent cholinergic innervation (Lewis & Shute, 1967; Mesulam *et al.* 1983). A wide range of cholinergic actions have been demonstrated in pyramidal neurons in rat and guinea-pig hippocampus and cortex; prominent among them are indirect muscarinic hyperpolarizations (Benardo & Prince, 1982; McCormick & Prince, 1986), direct muscarinic depolarizations (Benson, Blitzer & Landau, 1988; Dutar & Nicoll, 1988), muscarinic reduction in the slow after-hyperpolarization (AHP) that follows a train of action potentials (Benardo & Prince, 1982; Cole & Nicoll, 1984; Dutar & Nicoll, 1988) and its underlying potassium conductance ($I_{AHP}$, Constanti & Sim, 1987; Madison, Lancaster & Nicoll, 1987; Benson *et al.* 1988), blockade of the voltage-dependent potassium current $I_M$ (Benardo & Prince, 1982; Halliwell & Adams, 1982; Madison *et al.* 1987; Dutar & Nicoll, 1988), and suppression of a resting potassium leak conductance (Benardo & Prince, 1982; Madison *et al.* 1987; Benson *et al.* 1988). In addition, cholinergic reductions in excitatory postsynaptic potentials (Valentino & Dingledine, 1981; Dodt & Misgeld, 1986; Dutar & Nicoll, 1988) and inhibitory postsynaptic potentials (Haas, 1982) have been reported in these brain regions.

The purpose of the present study was to characterize the actions of cholinomimetics on neurons in the rat BLA and to compare these effects with those produced by synaptic release of ACh. To accomplish this, we sought first to characterize the physiological properties of pyramidal cells in the BLA in an *in vitro* slice preparation of rat ventral forebrain. In this way, we were able to target our study of cholinergic action on a physiologically identifiable and relatively homogeneous population of BLA cells. The results demonstrate both direct excitatory and indirect inhibitory cholinergic effects in pyramidal cells. The results also show that stimulation of endogenous release of ACh from cholinergic forebrain afferents in the slice mimics the effects of exogenous application of cholinomimetics. A preliminary report of these findings has appeared previously (Washburn & Moises, 1989).

## METHODS

Male Sprague–Dawley rats (Charles River) weighing 150–250 g were used in this study. Animals were killed by decapitation and their brains quickly removed and placed in ice-cold oxygenated artificial cerebrospinal fluid (ACSF), consisting of (in mM): NaCl, 124; KCl, 3·5; $MgSO_4$, 1·5; $NaH_2PO_4$, 26·2; glucose, 11·0 and $CaCl_2$, 3·0. Horizontal slices of ventral forebrain containing the amygdala were cut at a thickness of 450 $\mu$m using a Vibroslicer. One slice was transferred immediately to the recording chamber and held submerged between two layers of nylon mesh under continuously flowing ACSF pre-warmed to 32 °C. The remaining slices were transferred to an incubation chamber and maintained in oxygenated ACSF at room temperature. Slices were allowed to equilibrate for at least 1 h before intracellular recordings were attempted.

Conventional intracellular voltage recordings were obtained from cells in the BLA using glass microelectrodes filled with 2 M-potassium acetate (pH = 7·0) and having resistances of 90–160 M$\Omega$. In a small number of experiments, recordings were obtained with microelectrodes filled with one of the following solutions as electrolyte: 2 M-potassium chloride (KCl), 2 M-caesium acetate, 2 M-potassium acetate with 0·2 M-ethyleneglycol-bis-($\beta$-aminoethyl ether)-*N*,*N*,*N*,*',N'*-tetraacetic acid (EGTA) or 2 M-potassium acetate with 100 mM-cyclic AMP. Recordings of membrane voltage were amplified and displayed on an oscilloscope and chart recorder. Signals were also fed to a computer interface (TL-1, Axon Instruments) which digitized the analog waveforms for analysis by a microcomputer-based program (PClamp, Axon Instruments).

Only cells with membrane potentials more negative than $-55$ mV and overshooting action potentials were used in this study. Under our recording conditions the vast majority of BLA neurons were not spontaneously active. Cells were made to fire by passage of direct depolarizing current pulses through the recording electrode using a standard bridge-balance circuit (Axoprobe 1-A, Axon Instruments). Input resistance was determined by passing an incremental series of 150 ms current pulses (0·1 nA increments, range $-0·8$ to $+0·1$ nA; 150 ms) through the recording electrode and measuring the resultant voltage deflections. Current–voltage plots were then constructed by plotting the amplitude of each deflection against the amplitude of the corresponding current pulse. The slope of the line representing a linear regression of these points was taken to be the input resistance. Membrane time constants were calculated for small hyperpolarizing current pulses ($-3·0$ to $-0·2$ nA) using a least-squares fit exponential fitting program (Clampfit, Axon Instruments).

Excitatory and inhibitory postsynaptic potentials (EPSPs and IPSPs) were elicited by delivery of stimuli (voltage pulses of 0·1 ms duration) via a bipolar stimulating electrode placed on the surface of the slice in the external capsule (EC). Typically, the intensity of the stimulus delivered was adjusted so as to evoke an EPSP whose size was just below threshold for generating an action potential when the cell was held at its resting membrane potential. Membrane potential was manually adjusted by intracellular injection of DC current through the recording electrode and was held at $-80$ to $-90$ mV when eliciting EPSPs and held near threshold for firing (approximately $-60$ mV) when recording IPSPs. Activation of cholinergic afferents in the slice was accomplished by brief tetanic stimulation to the substantia inominata (SI) or EC, delivered at 30 Hz for 500 ms, using 0·1 ms stimuli. While the EC could be easily identified visually, we relied on anatomical landmarks in the slice and diagrams of stereotaxically defined sections (Paxinos & Waston, 1986) for guiding the placement of the recording electrode in the BLA and positioning of the stimulating electrode in SI.

To quantify the actions of cholinomimetics on the slow AHP that follows a series of current-evoked action potentials, samples of four to twelve digitized waveforms taken before, during and after drug application were averaged for each condition. From these averaged records, the area of the AHP was then calculated by integrating with respect to time the potential falling below baseline. The lower and upper limits utilized for the integration of the AHP were, respectively, the time following the current pulse at which the potential fell below the pre-pulse level, and the time at which the potential returned to the pre-pulse level.

Drugs were applied to the slice by switching the bath superfusate from normal ACSF to medium containing known concentrations of drug or by pressure ejection (typically 10–50 ms, 200 kPa) from a drug-containing extracellular pipette whose tip was placed at the slice surface near the recording electrode. The pipette tips were broken back to the desired diameter under visual observation and the pipettes filled with a drug solution of known concentration prepared in ACSF. Drugs used in this study were: acetylcholine chloride, carbamyl chloride (carbachol), oxotremorine, methacholine, atropine sulphate, pirenzepine, dimethylpiperidinium chloride (DMPP), hexamethonium chloride, tetraethylammonium (TEA), Lucifer Yellow CH (dilithium salt) (all obtained from Sigma Chemical Co.) and muscarine and oxotremorine-M (each from Research Biochemicals Inc.). McN-A-343 was a gift from Dr Stephen Fisher (University of Michigan). In some experiments, tetrodotoxin (TTX; Sigma) was included in the bathing medium to block action potential-dependent neurotransmitter release, thereby enabling us to distinguish direct actions of drugs on the neuron under study from possible remote actions.

For intracellular labelling, electrodes were filled with 4 % Lucifer Yellow CH (Sigma) in 1 M-lithium acetate. These electrodes typically had resistances between 120 and 300 M$\Omega$. No drug data were obtained from these cells due to the level of noise in the recordings and possible confounding effects arising from intracellular actions of lithium. After characterization of passive and active membrane properties, neurons were dye-filled by passing 0·5–1·0 nA hyperpolarizing constant current for 1–15 min. Brain slices containing Lucifer Yellow-filled cells were fixed overnight in 4 % paraformaldehyde and then stored up to 1 week in Tris-buffered saline solution at 4 °C. Slices were then dehydrated in alcohol and cleared in methyl salicylate. Cells were observed and photographed using a Leitz Orthoplan microscope. Camera lucida drawings were also made of representative cells.

RESULTS

Cholinergic actions were examined in 296 BLA neurons from which long-term stable intracellular recordings were obtained. The results presented here primarily deal with the responses of neurons that were classified as pyramidal-type cells based on electrophysiological criteria and subsequent morphological characterization with Lucifer Yellow. Previous studies involving Golgi impregnation or immunohistochemical labelling of neurons in rat BLA have revealed that greater than 95% of all neurons are pyramidal in nature and possess morphological features remarkably similar to those of pyramidal neurons that are found in the hippocampus or neocortex (McDonald, 1982, 1984; Millhouse & DeOlmos, 1983). In keeping with this, greater than 93% of all the impalements that were obtained in this study were made from neurons which displayed a uniform profile of passive and active electrophysiological properties (see below). In addition, intracellular Lucifer Yellow labelling of seventy-eight neurones following their electrophysiological characterization confirmed that the cells described here were pyramidal in nature. A typical example of a Lucifer Yellow-labelled BLA pyramidal neuron is shown in Fig. 1A. Pyramidal cells in the BLA usually possessed a distinctive prominent apical dendrite and thinner basal dendrites and, with the exception of perisomatic regions, all dendritic processes were densely covered with spines. The apical dendrite was most often found to be oriented in a rostral direction. These findings are in keeping with the results of earlier anatomical work in which the Golgi method was used to examine cellular morphology in rat BLA (McDonald, 1982, 1984; Millhouse & DeOlmos, 1983).

The pyramidal cells included in this study constituted a rather homogeneous population in terms of their physiological properties and, as such, could be distinguished electrophysiologically from other classes of neurons that are found in rat BLA (see Washburn & Moises, 1990). A representative sampling of pyramidal cells revealed that they had a mean resting membrane potential of $-69.5 \pm 0.7$ mV ($\pm$ s.e.m., $n = 85$), input resistance of $39.5 \pm 1.6$ M$\Omega$ ($n = 46$) and a time constant of $15.7 \pm 0.7$ ms ($n = 44$) (see Fig. 1Ba). The mean duration of the action potential, as measured at its base, was $1.9 \pm 0.2$ ms ($n = 36$) and the spike amplitude averaged $92.0 \pm 2.0$ mV ($n = 27$) when evoked from resting membrane potential.

Under our experimental conditions, pyramidal neurons were not spontaneously active at resting membrane potential but could be made to fire by intracellular injection of a depolarizing current pulse through the recording electrode. Passage of a short (10 ms) depolarizing current pulse that was just above threshold for spike generation caused the cell to fire a single action potential followed by a small depolarizing after-potential (arrow in Fig. 1Bb, trace 2, left). Delivery of a slightly larger depolarizing pulse increased the size of the after-potential and characteristically led to the generation of a second spike that was of longer duration than the initial spike (Fig. 1Ba and 1Bb, right). In response to passage of a prolonged (300–450 ms) depolarizing current pulse, these neurons discharged an initial burst or short train of spikes whose discharge frequency declined over 100–200 ms and in some cases then fell silent throughout the remainder of the depolarizing command (Figs 1B and C and 2Bb, left panel). While nearly all cells showed some degree of accommodation in spike discharge to a prolonged depolarizing stimulus, a majority
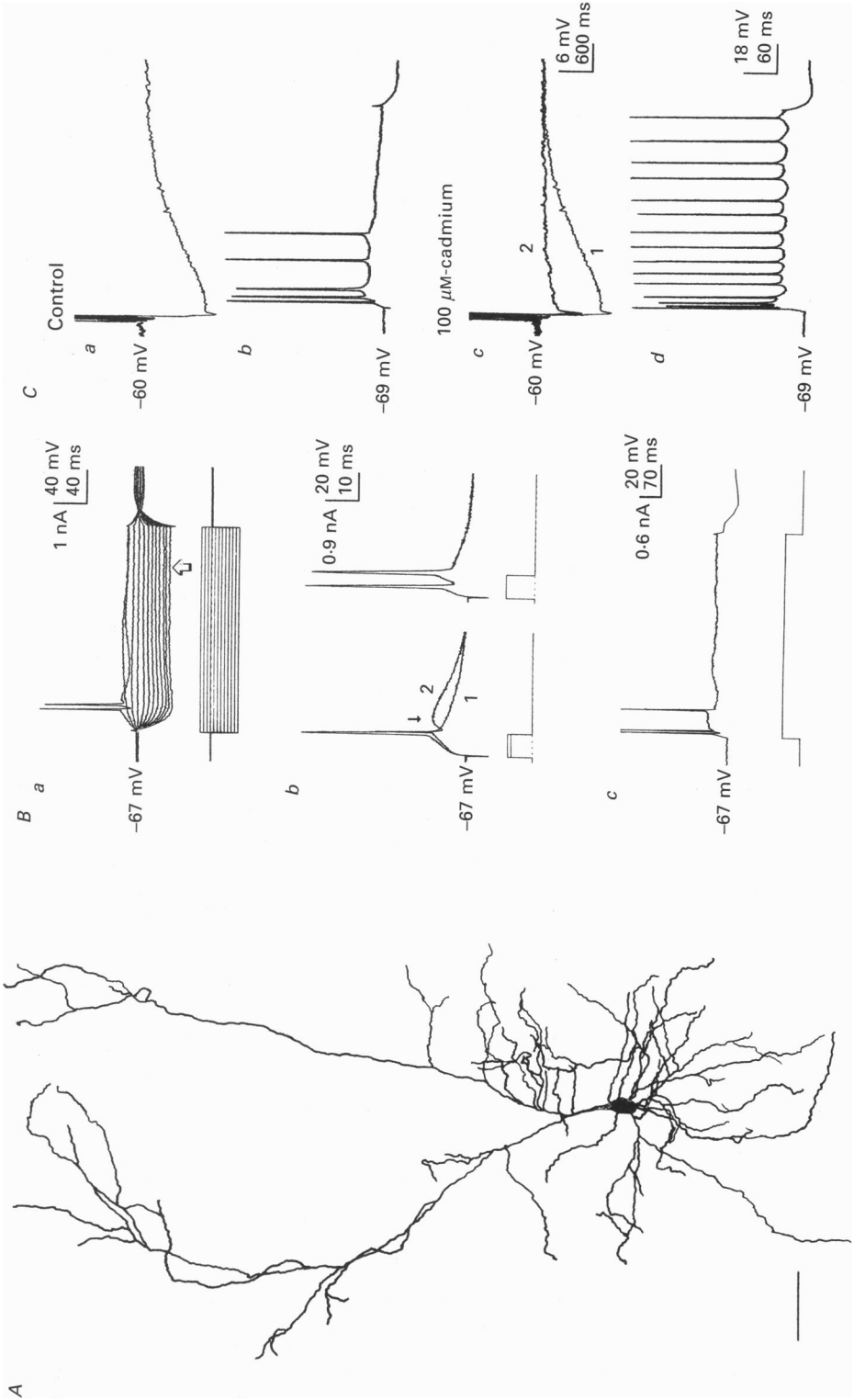
Fig. 1. For legend see facing page.

of the neurons (65%) showed a progressive slowing in their rate of spike discharge over the course of current injection, without a complete cessation of firing.

In most BLA pyramidal neurons, an after-hyperpolarization (AHP) followed a current-evoked burst of action potentials after termination of the depolarizing command, as has been reported previously (Gean & Shinnick-Gallagher, 1989). These hyperpolarizing events were composed of two readily distinguishable components: an initial event having a time course of tens of milliseconds (referred to here as the medium AHP) and a slow component which lasted for up to seconds. It should be noted that the early phase of the medium AHP was likely to include a fast AHP (2–5 ms duration) which followed individual action potentials (for example, see Fig. 1$Bb$, left panel). Studies in hippocampal pyramidal cells indicate that the medium AHP is a complex potential mediated by the combined effects of the anomalous rectifier current, $I_Q$, the voltage-dependent potassium current, $I_M$, and the calcium-dependent potassium current, $I_C$ (Storm, 1989; Williamson & Alger, 1990). A separate calcium-dependent potassium current, $I_{AHP}$, appears to underlie the slowly developing AHP (Lancaster & Nicoll, 1987; Madison et al. 1987) and accounts for the accommodation properties of these neurons (Madison & Nicoll, 1984; Lancaster & Nicoll, 1987). The slow AHP and accommodation responses of BLA pyramidal neurons reported here also appeared to be due to a calcium-activated potassium conductance, as demonstrated by blockade of these events by bath application of the calcium channel antagonist cadmium (100 $\mu$M, $n = 4$) (Fig. 1$C$) or intracellular injection of the potassium channel blocker caesium (2 M, $n = 6$) or the calcium-chelating agent EGTA (0·2 M in 2 M-potassium acetate, $n = 5$) (data not shown). In addition, we found that low concentrations of the potassium channel blocker TEA (0·2–1 mM, $n = 5$) reduced only the medium AHP whereas bath application of

---

Fig. 1. *A*, camera lucida reconstruction of a Lucifer Yellow-filled BLA pyramidal cell. Note pyramidal-type soma with prominent apical dendrite and large number of basal dendrites. Dendritic spines are not illustrated. Calibration bar represents 50 $\mu$m. *B*, membrane characteristics of a typical BLA pyramidal neuron. *Ba*, superimposed traces showing the intracellular responses to hyperpolarizing and depolarizing current pulses (−0·8 to +0·3 nA in 0·1 nA steps). Note the slight sag in the response to the largest hyperpolarizing pulse (open arrow) and the two-spike burst in response to a suprathreshold depolarizing current pulse. *Bb*, action potential generation in response to short current pulses. Intracellular injection of depolarizing current which was subthreshold for action potential generation (0·7 nA, 10 ms) elicited an electrotonic potential which decayed back to resting level (trace 1). A depolarizing after-potential (arrow) followed the action potential elicited by delivery of a current pulse (0·8 nA) which was just large enough to trigger a spike (trace 2). With a slightly larger pulse (0·9 nA), the after-potential was large enough to evoke a second spike (right). *Bc*, spike frequency accommodation properties. The cell fired a two-spike burst followed by a single action potential in response to prolonged (450 ms) depolarizing current (0·5 nA). Resting membrane potential was −67 mV. *C*, reduction by cadmium of the current-evoked after-hyperpolarization (AHP) and spike frequency accommodation in another pyramidal cell. *Ca*, intracellular injection of a 150 ms depolarizing current pulse (1·0 nA) elicited a burst of action potentials followed by a multiphasic AHP. *Cb*, this cell showed accommodation of spike discharge during delivery of a 450 ms depolarizing (0·5 nA) command. *Cc* and *Cd*, the AHP was reduced and accommodation was blocked by superfusion of cadmium-containing medium. For purposes of comparison, the control AHP response (trace 1 in *Cc*) is superimposed on the response elicited in the presence of cadmium (trace 2). Resting membrane potential was −69 mV. Recordings in this and subsequent figures were obtained with 2 M-potassium acetate-filled electrodes, unless otherwise noted.
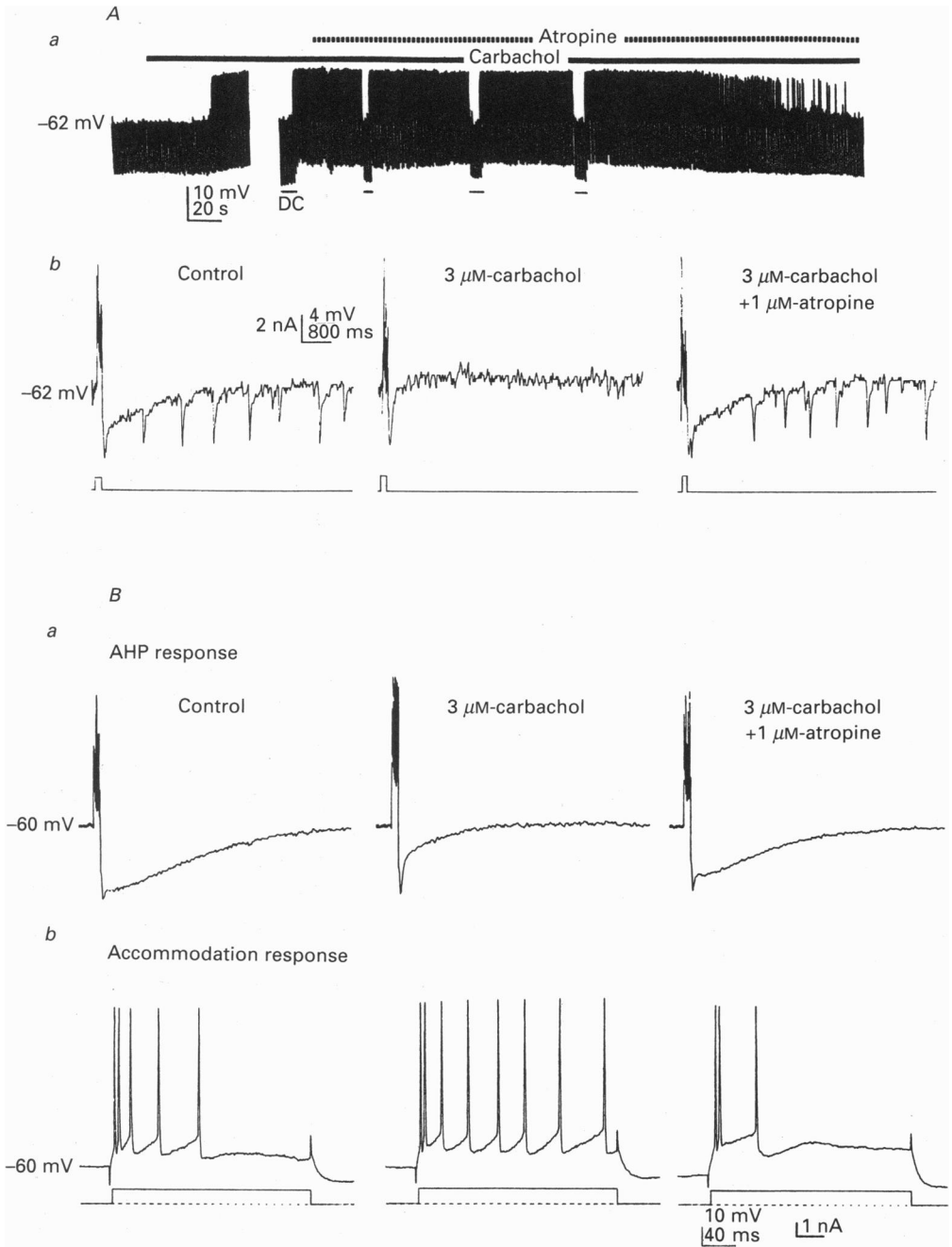
Fig. 2. Effect of carbachol on membrane potential, after-hyperpolarizations (AHPs) and the accommodation response in BLA neurons. $A\,a$, chart record shows that superfusion of carbachol ($3\,\mu$M) produced a strong depolarization when applied at resting membrane potential ($-62$ mV). Large downward deflections in the voltage record in this and subsequent figures are electrotonic potentials elicited by passage of constant current hyperpolarizing pulses through the recording electrode. The carbachol-induced depolarization was reversed when atropine ($1\,\mu$M) was added to the bathing medium. Break

8-bromo-cyclic AMP (1 mM, $n = 4$) or intracellular injection of cyclic AMP (100 mM, $n = 3$) eliminated the slow AHP while having little or no effect on the medium AHP (data not shown). These results support the conclusion that the AHPs recorded in rat BLA neurons are similar to those found in other pyramidal-type neurons in the brain.

*Superfusion of cholinergic drugs*

Bath application of the cholinergic agonist carbachol had marked effects on the excitability of BLA pyramidal neurons. While cholinergic responsiveness was routinely assessed using carbachol at a concentration of 3 μM, the effects of the agonist could be seen at concentrations as low as 100 nM and all the agonist-induced effects described here were concentration dependent. The records in Fig. 2 illustrate a number of the major effects that were produced by superfusion of carbachol in BLA pyramidal neurons. The first of these was a slow membrane depolarization that in many cases was large enough to cause repetitive firing (Fig. 2*Aa*). The depolarization was associated with an increase in input resistance, which was determined by passing constant current hyperpolarizing pulses through the recording electrode. This increase in input resistance was seen more clearly when a steady hyperpolarizing current was applied through the electrode to return the membrane potential back to resting level (see bar labelled DC in Fig. 2*Aa*). These depolarizations appeared to be voltage dependent in that they occurred only in cells that had resting membrane potentials more positive than $-65$ mV or in neurons whose membrane potential had been manually depolarized to near firing threshold by intracellular injection of DC current prior to agonist superfusion. Bath application of carbachol (3 μM) or the muscarinic agonists muscarine (3–10 μM, $n = 4$) or oxotremorine-M (3–10 μM, $n = 7$) produced slow depolarizing responses in thirty-seven of 208 cells when recording at resting membrane potential. The relatively low incidence of cholinergic responses appeared to reflect the voltage-dependent nature of these events, since application of carbachol or muscarinic agonists during depolarization of the membrane to just below firing threshold with DC current produced depolarization in twenty-two of thirty-one neurons which failed to respond at their resting membrane potential. The depolarizing effect of carbachol (3 μM) was fully reversed by the muscarinic antagonist atropine (1 μM) (Fig. 2*Aa*), but not by the nicotinic antagonist hexamethonium, indicating its mediation via a muscarinic-type receptor.

The second major cholinergic action on BLA pyramidal neurons was a reduction in the slow component of the AHP that followed a current-evoked burst of action potentials (Fig. 2*Ab*). Carbachol reversibly reduced the slow AHP with an $IC_{50}$

in the chart record represents 3 min. *A b*, in the same cell, passage of a 150 ms depolarizing current pulse (1·0 nA) through the recording electrode caused the cell to fire a burst of action potentials followed by a medium and slow AHP (left). Administration of carbachol blocked the slow AHP but not the medium AHP (middle) and this effect was reversed in the presence of atropine (right). Note that carbachol also blocked the occurrence of spontaneous inhibitory synaptic potentials, which appear as phasic hyperpolarizing events in the decay phase of the AHP. *B*, recording from a different cell illustrates the reduction in the slow AHP by carbachol (*Ba*) and concomitant blockade of spike frequency accommodation (*Bb*). Each of these effects was reversed by atropine (right panels). Resting membrane potential was $-69$ mV.

(concentration giving 50% maximal inhibition) of approximately 500 nM (Fig. 3) and this effect occurred independent of changes in action potential duration or in the amplitude of the medium AHP. In virtually all cases, the reduction of the slow AHP was associated with a concomitant reduction of spike frequency accommodation, as
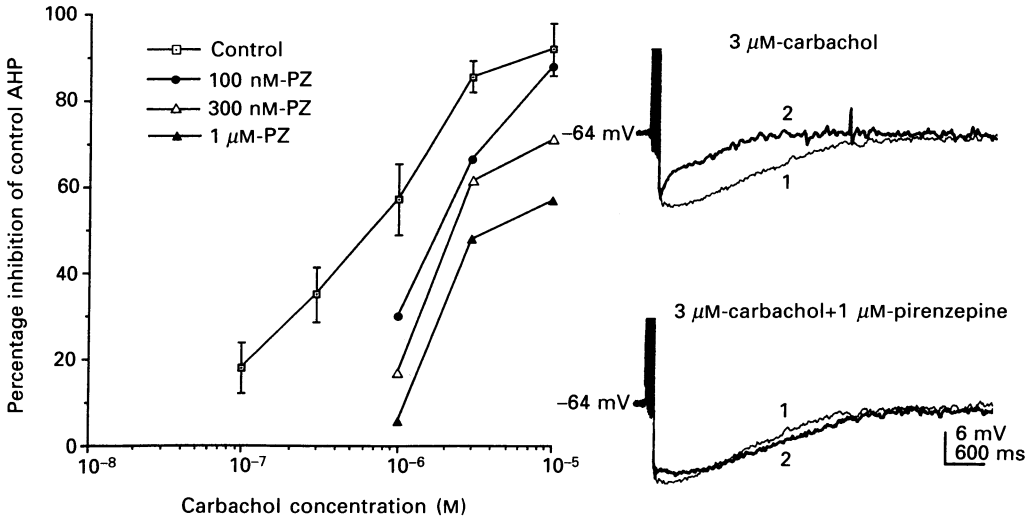


Fig. 3. *A*, dose–response curves for reduction of the slow AHP by carbachol generated in the absence (control) and presence of increasing concentrations of pirenzepine (PZ) (0·1–1·0 μM). Pirenzepine produced a parallel, rightward shift in the carbachol dose–response curve. Each data point represents the mean ±s.e.m. of determinations in six to thirteen neurons. For purposes of clarity, error bars were omitted from the curves generated in the presence of the antagonist. *B*, records from a typical experiment showing the depressant effect of carbachol on the slow AHP and its reversal by pirenzepine. In each record, the control AHP recorded in the absence of drug (trace 1) is superimposed on the response elicited under the indicated drug conditions (trace 2). Resting membrane potential was −64 mV.

shown for example in Fig. 2*Bb*. While the blockade of the slow AHP and accommodation by carbachol occasionally occurred in association with the generation of the cholinergic slow depolarization (see records from cell shown in Fig. 2*A*), such effects were characteristically observed in the absence of any change in membrane potential (e.g. Fig. 2*B*). The reduction of the slow AHP and spike frequency accommodation by carbachol was blocked by low concentrations of atropine (0·1–1·0 μM, $n = 16$) (Figs. 2*A* and *B*, right panels) but not by hexamethonium (10–50 μM, $n = 8$). In addition, both actions of carbachol were mimicked by superfusion of muscarine (1–10 μM, $n = 8$), oxotremorine (1 μM, $n = 3$) and oxotremorine-M (1 μM, $n = 8$), but not by the nicotinic agonist DMPP (10 μM, $n = 5$), consistent with their mediation via a muscarinic receptor. Previous studies have suggested that the $M_1$ receptor is involved in the muscarinic reduction of the AHP in hippocampal pyramidal cells (Dutar & Nicoll, 1988) and myenteric plexus neurons (Galligan, North & Tokimasa, 1989). Similarly, in experiments utilizing the $M_1$-selective antagonist pirenzepine, we were able to demonstrate a dose-dependent, competitive antagonism of the carbachol-induced reduction of the slow AHP in BLA pyramidal cells (Fig. 3).

We examined the effect of carbachol on the calcium action potential to determine whether a reduction in calcium entry could account for the reduction of the slow AHP. When recordings were made in the presence of TTX (1 $\mu$M) and TEA (5 mM), passage of a brief (150 ms) depolarizing current pulse through the recording electrode caused the cell to fire a calcium spike (Fig. 4*B*, lower left panel) followed by a medium and slow AHP (Fig. 4*A*, upper left panel). At a time when carbachol (10 $\mu$M) had substantially reduced the slow component of the AHP, the calcium spike was largely undiminished in size and was, in fact, slightly broadened (cf. Fig. 4, centre panels). The recordings in Fig. 4 also show that a TEA-insensitive component of the medium AHP was largely unaffected by carbachol. Similar results were obtained in three additional neurons and in all four cases, the inhibitory effect of carbachol on the slow AHP was blocked by atropine (500 nM–1 $\mu$M) (Fig. 4, right panels) and mimicked by muscarine (3 $\mu$M, $n = 2$).

In many neurons, the reduction of the slow AHP by carbachol was accompanied by a depolarizing after-potential (DAP) that typically appeared to emerge from the decay phase of the muscarinic-insensitive medium AHP. The amplitude of the DAP increased with elevations in the concentration of bath-applied carbachol, and also when recordings were obtained as the cell was progressively depolarized during passage of DC current. Measurements taken in the presence of carbachol (3 $\mu$M) revealed that the DAP had a mean extrapolated reversal potential of $-81{\cdot}5 \pm 1{\cdot}6$ mV ($n = 13$) and duration of $6{\cdot}9 \pm 0{\cdot}4$ s ($n = 9$) when recordings were made at a membrane potential of $-65$ mV. When carbachol was applied to cells that were held just below threshold for firing (approximately $-60$ mV) with DC current, the DAP was large enough to depolarize the cell above threshold and trigger firing that could last several minutes. In addition, in many neurons in which carbachol had no effect on resting membrane potential, the after-potential elicited by periodic intracellular current injection ($0{\cdot}5$–$1{\cdot}0$ nA at $0{\cdot}07$–$0{\cdot}2$ Hz) summated in a stepwise fashion to produce large (10–20 mV) depolarizations. It should be noted that DAPs having properties similar to those observed here have been described previously following muscarinic receptor activation in guinea-pig hippocampal (Benardo & Prince, 1982) and cortical (McCormick & Prince, 1986) pyramidal cells.

A third prominent effect of carbachol that was observed in BLA pyramidal neurons was a reduction in the frequency and amplitude of spontaneous and stimulus-evoked synaptic potentials. For example, in the records shown in Fig. 2*Ab*, spontaneous IPSPs are seen as the large downward deflections throughout the decay phase of the AHP that follows a current-evoked burst of spikes. These spontaneous inhibitory events were eliminated during superfusion of 3 $\mu$M-carbachol (Fig. 2*Ab*, middle panel) and reappeared after switching to medium containing carbachol (3 $\mu$M) and atropine (1 $\mu$M) (Fig. 2*Ab*, right panel). Muscarinic blockade of spontaneous IPSPs was typically not associated with any change in membrane potential. This finding suggests that the removal of tonic inhibitory input by carbachol was unlikely to account for muscarinic depolarizations recorded at the soma.

Excitatory and inhibitory synaptic potentials that were elicited in BLA neurons following stimulation of afferents within the EC were also reduced by bath application of carbachol or muscarinic agonists. Electrical stimulation of the EC routinely produced an EPSP at short latency (Fig. 5*A*, left panel) followed by an
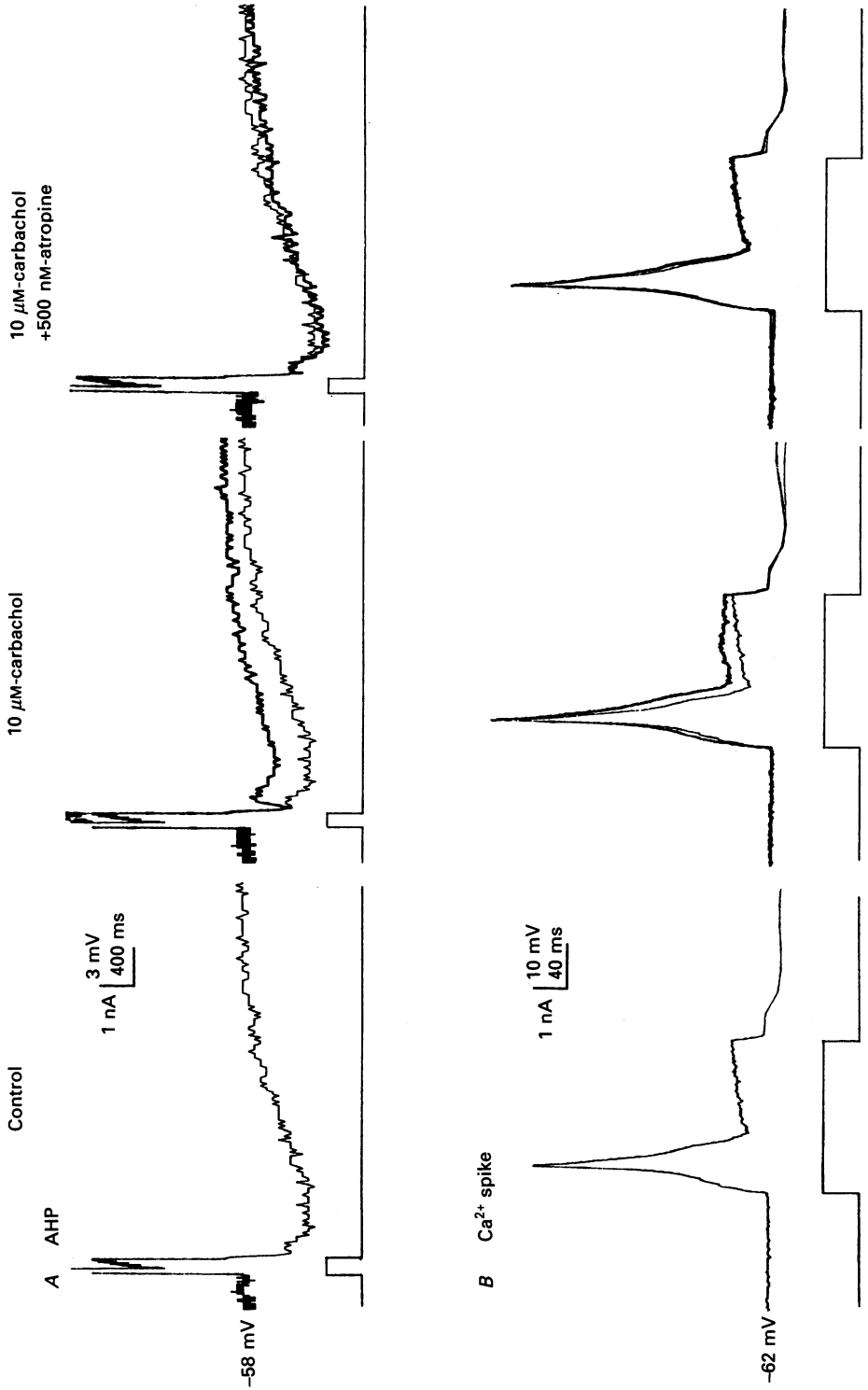
A  AHP

Control

10 μM-carbachol

10 μM-carbachol
+500 nM-atropine

1 nA | 3 mV
400 ms

−58 mV

B  Ca²⁺ spike

1 nA | 10 mV
40 ms

−62 mV

Fig. 4. For legend see facing page.

early IPSP which reached peak amplitude $37 \pm 1.6$ ms ($n = 46$) following stimulation. As the stimulation intensity was increased, the early IPSP was followed by a late IPSP which reached maximal amplitude at $171 \pm 2.6$ ms ($n = 44$) and lasted from 700–1000 ms (Fig. 5*B*, left panel). Carbachol reduced the amplitude of the stimulus-evoked fast EPSP in a concentration-dependent manner ($IC_{50}$ of approximately 10 $\mu$M) and, in nearly all cases examined (152 of 159 cells), this effect was associated with concomitant reductions in the early and late IPSPs (Fig. 5). These effects occurred independent of changes in resting membrane potential or input resistance of the cell and showed reversal within 20 min after switching from drug-containing ACSF to normal bathing medium. The inhibitory effects of carbachol on the stimulus-evoked postsynaptic potentials were blocked by atropine (0·1–1·0 $\mu$M, $n = 12$) (Fig. 5, right panels) but not by hexamethonium (10–50 $\mu$M, $n = 5$) and were mimicked by muscarine (1–3 $\mu$M, $n = 4$) and oxotremorine-M (1 $\mu$M, $n = 5$) but not DMPP (10 $\mu$M, $n = 3$). These results indicate that the cholinergic reduction of synaptic events in the BLA results from the activation of muscarinic-type receptors.

We examined the responses of BLA neurons to pressure application of GABA or baclofen before, during and after bath application of carbachol to determine whether the cholinergic reduction in the early and late IPSPs might reflect changes in postsynaptic chemosensitivity to inhibitory neurotransmitter. Local application of GABA (3 mM) to the surface of the slice near the recording electrode elicited a triphasic response profile (Fig. 5*A*, insets), consisting of an initial hyperpolarization and subsequent depolarization that are mediated by an increase in chloride conductance, followed by a late hyperpolarization mediated by an increase in potassium conductance (see Moises & Washburn, 1989). The triphasic profile of the GABA-induced response was unaffected during superfusion of carbachol (3 $\mu$M) at a time when the early and late IPSPs elicited by EC stimulation were clearly reduced, as shown by the insets in Fig. 5*A*. Pressure application of the $GABA_B$ agonist baclofen (3 mM) to the slice produced only hyperpolarizations in BLA pyramidal neurons and these responses were similarly unaffected by carbachol (3–10 $\mu$M, $n = 6$, data not shown).

*Responses to local application of cholinergic drugs*

To further examine cholinergic actions in the BLA, carbachol and other cholinomimetics were applied to the surface of the slice from an extracellular pipette in order to limit the duration of drug action and better localize the site of drug effect. Brief applications of carbachol (10 ms duration at 200 kPa, 3 mM concentration in

Fig. 4. Effect of carbachol on the slow AHP and calcium spikes in a BLA pyramidal cell. All recordings were obtained in the presence of 1 $\mu$M-TTX and 5 mM-TEA. *A*, traces represent the AHPs which follow the calcium action potential elicited by passage of a short depolarizing current pulse through the recording electrode (1 nA, 150 ms). The middle panel shows the AHP elicited following bath perfusion of carbachol (10 $\mu$M) for 15 min. In the centre and right columns of this figure, responses recorded in the presence of drug (thick lines) are superimposed on the control response (thinner lines). The record on the right was obtained 15 min after switching to ACSF containing carbachol (10 $\mu$M) and atropine (500 nM). *B*, the top records are expanded portions of the traces from *A* and show the corresponding calcium spikes recorded under control conditions (left) and during perfusion of carbachol in the absence (middle) and presence of atropine (right). Resting membrane potential was $-72$ mV).
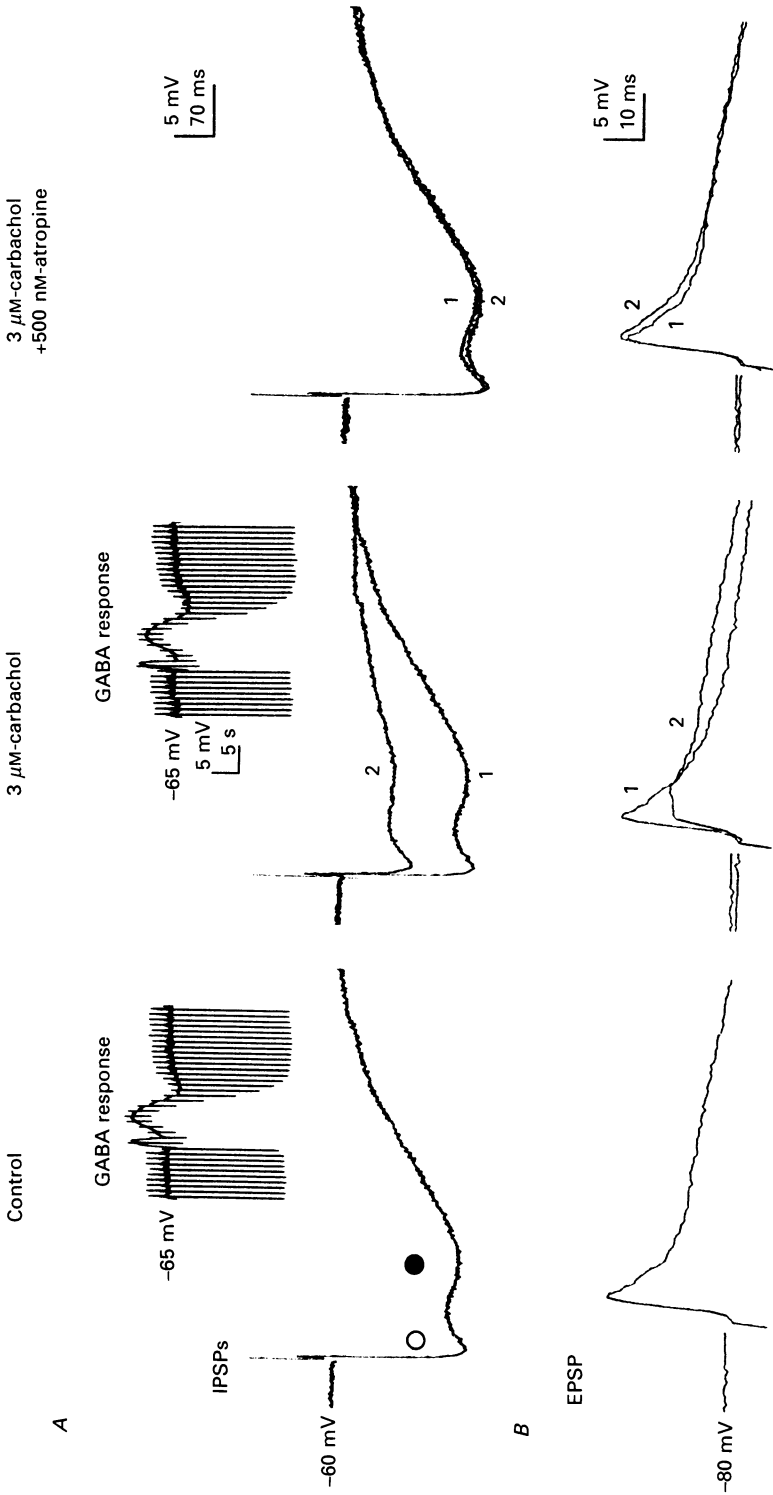
Fig. 5. Carbachol-induced depression of the non-cholinergic EPSP and IPSPs elicited in a BLA pyramidal cell following external capsule (EC) stimulation. A, when the cell was depolarized to −60 mV with intracellular current injection, electrical stimulation of the EC elicited an EPSP followed by an early (○) and late IPSP (●). Inset shows depolarizing and hyperpolarizing responses of the same cell to 20 ms pressure ejection of GABA (10 μM) that are recorded at a membrane potential of −65 mV. Supertusion of carbachol (middle panels) reduced both the early and late IPSPs in an atropine-sensitive manner, whereas the response to GABA was unchanged (inset). Trace 1 in middle and right panels represents the control response, whereas trace 2 corresponds to the response in carbachol (centre) and in the presence of carbachol and atropine (right). B, in the same cell, the EPSP evoked by EC stimulation was also reduced by carbachol and this effect was reversed by atropine. Resting membrane potential was −69 mV.

the pipette) mimicked the profile of effects obtained during bath superfusion of the agonist, producing slow depolarizations in pyramidal cells, blockade of the slow AHP and spike frequency accommodation and reductions in spontaneous and synaptically evoked postsynaptic potentials. However, while slightly less than 20 % of BLA pyramidal neurons were found to respond to bath administration of carbachol with changes in membrane potential, in virtually all cells (ninety of ninety-six cases), local application of drugs elicited a stereotyped biphasic membrane response consisting of a rapid hyperpolarization followed by a prolonged depolarization. It should be noted that such biphasic responses were occasionally observed during bath superfusion of drugs but could only be elicited with high agonist concentrations (e.g. carbachol in excess of 30 $\mu$M).

Agonists and antagonists having selectivity for muscarinic and nicotinic receptors were used to characterize the cholinergic receptor mediating the depolarizing and hyperpolarizing effect of carbachol on membrane potential. Bath application of atropine (0·1–1·0 $\mu$M) reversibly blocked the carbachol-induced hyperpolarization and depolarization in all eighteen BLA pyramidal neurons tested, whereas administration of the nicotinic antagonist hexamethonium at concentrations as high as 50 $\mu$M had no effect on either of these membrane responses ($n = 7$). The conclusion that the depolarizing and hyperpolarizing responses to carbachol resulted from the activation of muscarinic receptors received added support from the finding that local application of the muscarinic agonists oxotremorine-M (5–10 mM, $n = 12$) (Fig. 7), oxotremorine (10 mM, $n = 3$), muscarine (3 mM, $n = 6$), methacholine (10 mM, $n = 2$) or McN-A-243 (3 mM, $n = 6$) produced a similar profile of membrane hyperpolarization followed by a slow depolarization associated with an increase in input resistance. Conversely, tests in eight BLA neurons failed to reveal any effect of the nicotinic agonist dimethylpiperazinium (DMPP, 10 mM) on membrane potential, although small decreases in input resistance were occasionally observed.

The carbachol-induced hyperpolarization was typically less than 5 mV in amplitude when recording at resting membrane potential (mean = $3·6 \pm 0·4$ mV, $n = 24$) whereas it increased in size as the cell was depolarized with intracellular injections of DC current. Results in Fig. 6$A$ show that the hyperpolarizations to carbachol were associated with a decrease in membrane input resistance. To gain insight into the nature of these hyperpolarizing responses, we compared the reversal potential of this response to that of the chloride-mediated early IPSP that is recorded in BLA pyramidal cells following activation of amygdalopetal afferents within the EC (Moises & Washburn, 1989). This type of analysis is illustrated in Fig. 6. A plot of the amplitudes of the carbachol-induced hyperpolarizations (Fig. 6$A$) and early IPSPs ($\bullet$, Fig. 6$B$) elicited over a range of membrane potentials revealed that both responses had reversal potentials of approximately $-78$ mV (Fig. 6$C$). Overall, we found that there was close agreement between the reversal potential of the early IPSP ($-73·6 \pm 1·9$ mV, $n = 32$) and that of the initial hyperpolarization to carbachol pressure ejection ($-76·1 \pm 1·0$, $n = 25$), when determined in this manner.

In all cases ($n = 90$), the initial hyperpolarizing response to carbachol application was followed by a slow membrane depolarization. These depolarizing responses were of variable duration and were typically associated with an increase in input resistance (mean increase at $-60$ mV = $26·7 \pm 4·2$ %, $n = 16$), as determined by passing constant-current hyperpolarizing current pulses through the recording
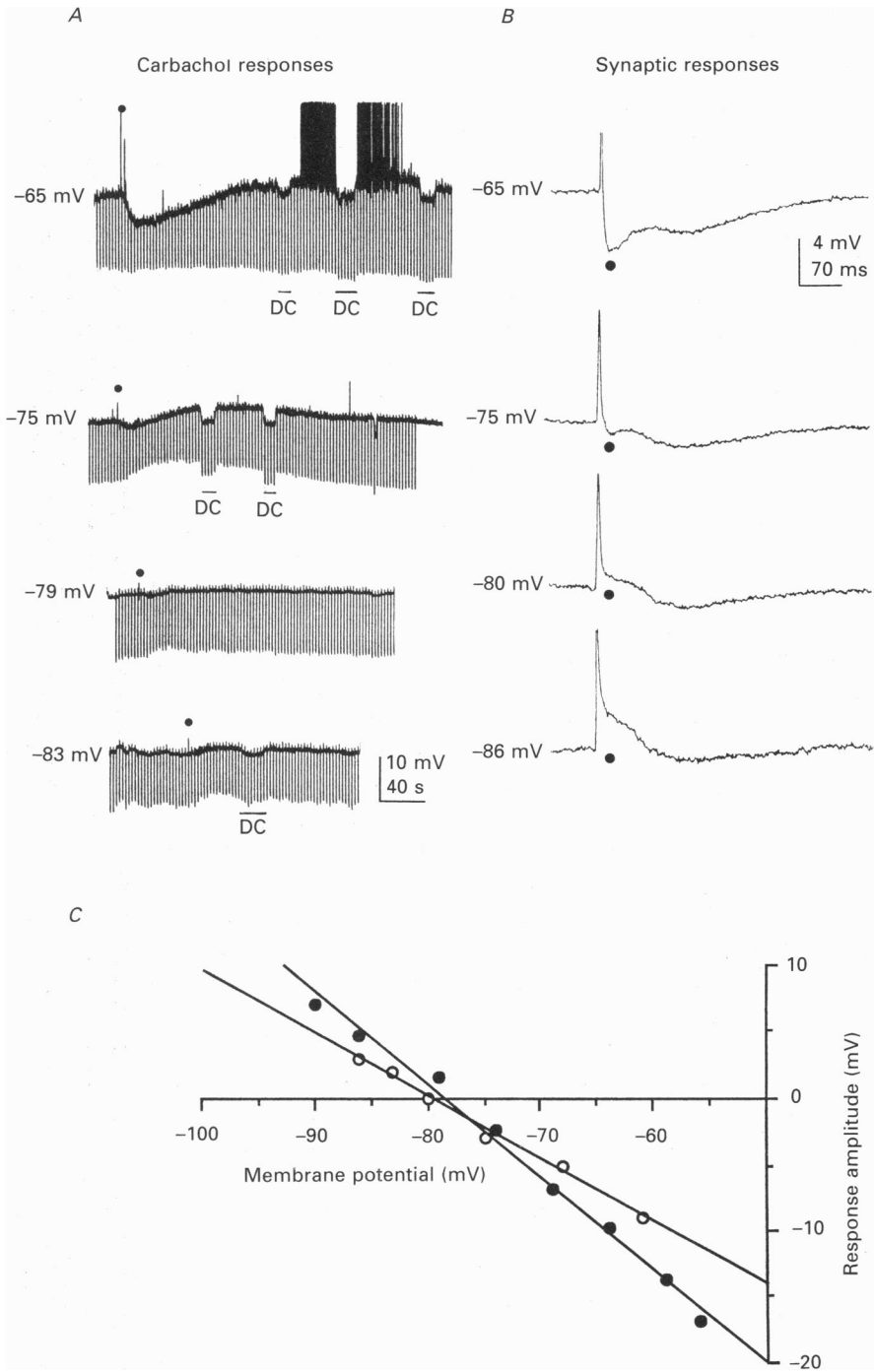
Fig. 6. Comparison of reversal potentials of the early IPSP and hyperpolarizing responses to local application of carbachol. *A*, chart records show responses to carbachol pressure ejection (10 ms, ●) recorded at various membrane potentials. *B*, digitized records illustrate the synaptic responses to stimulation of the EC that were recorded in this

electrode. The cholinergic depolarization was typically small when the agonist was applied at resting membrane potential (mean = $2\cdot3\pm0\cdot4$ mV, $n = 9$ from a mean resting membrane potential of $-70\cdot2$ mV), but increased in size when responses were elicited from more depolarized membrane potentials. For example, application of carbachol to neurons which were depolarized 10 mV from rest yielded slow depolarizations whose amplitude averaged $9\cdot8\pm1\cdot6$ mV ($n = 16$). Under these conditions, agonist applications which had produced small depolarizations at the cell's resting level often resulted in the generation of a continuous, high-frequency spike discharge that lasted up to 15 min. In a few neurons, a transient decrease in input resistance was observed during the initial phase of the depolarizing response (for example, see the response evoked from $-75$ mV in Fig. 6$A$). This was most probably attributable to the increase in membrane conductance associated with the preceding hyperpolarization, since it was not observed when GABA antagonists or TTX were included in the bath to prevent the carbachol-induced hyperpolarization (see below).

To determine the reversal potential of the carbachol-induced depolarization, we measured the amplitudes of the responses evoked by 10 ms applications of drug while systematically adjusting the membrane potential of the cell by intracellular injection of current. Results obtained from experiments on twenty-three neurons yielded two apparently different voltage sensitivities for this slow cholinergic depolarizing response. In twelve cases, carbachol elicited slow depolarizations only when cells were depolarized away from their resting level ($-70\cdot8\pm2\cdot2$ mV) to an average membrane potential of $-64\cdot3\pm0\cdot6$ mV. In contrast, in the remaining eleven neurons, cholinergic depolarizations did not show this form of voltage dependency. Instead, there was a progressive reduction in the amplitude of the responses as they were elicited from increasingly more hyperpolarized levels of membrane potential. In these neurons, the mean reversal potential for the depolarizing response was $-85\cdot4\pm1\cdot2$ mV, a value significantly hyperpolarized relative to resting membrane potential ($-69\cdot3\pm1\cdot8$ mV, $P < 0\cdot05$) and close to the estimated value of $E_K$ (reversal potential for K$^+$) determined for our recording conditions. The responses of the neuron depicted in Fig. 6$A$ are typical of this second group of cells.

Previous investigations indicate that the ionic mechanism underlying the cholinergic slow depolarizations in hippocampal and cortical pyramidal cells as well as a number of other neurons (for review see North, 1989) involves a decrease in a potassium leak conductance or a block of the voltage-dependent current $I_M$. In the experiment shown in Fig. 7, we examined the effect of altering the external potassium concentration on the depolarizing response to pressure ejection of the muscarinic agonist oxotremorine-M to determine whether the slow depolarizations in BLA pyramidal cells were mediated by a similar block of potassium conductance. In this cell, the amplitude of the depolarization to local application of oxotremorine-M was markedly reduced when the potassium concentration in the bathing medium was increased from the normal 3·5 to 7 mM. Similar results were obtained in four other

pyramidal cell from approximately the same membrane potentials. The early IPSP is indicated by ●. $C$, plots of the amplitudes of the early IPSP (●) and carbachol-induced hyperpolarization (○) against membrane potential. Regression lines through the data points yielded a reversal potential of $-78$ mV for the early IPSP and $-80$ mV for the hyperpolarizing response to carbachol. Resting membrane potential was $-72$ mV.
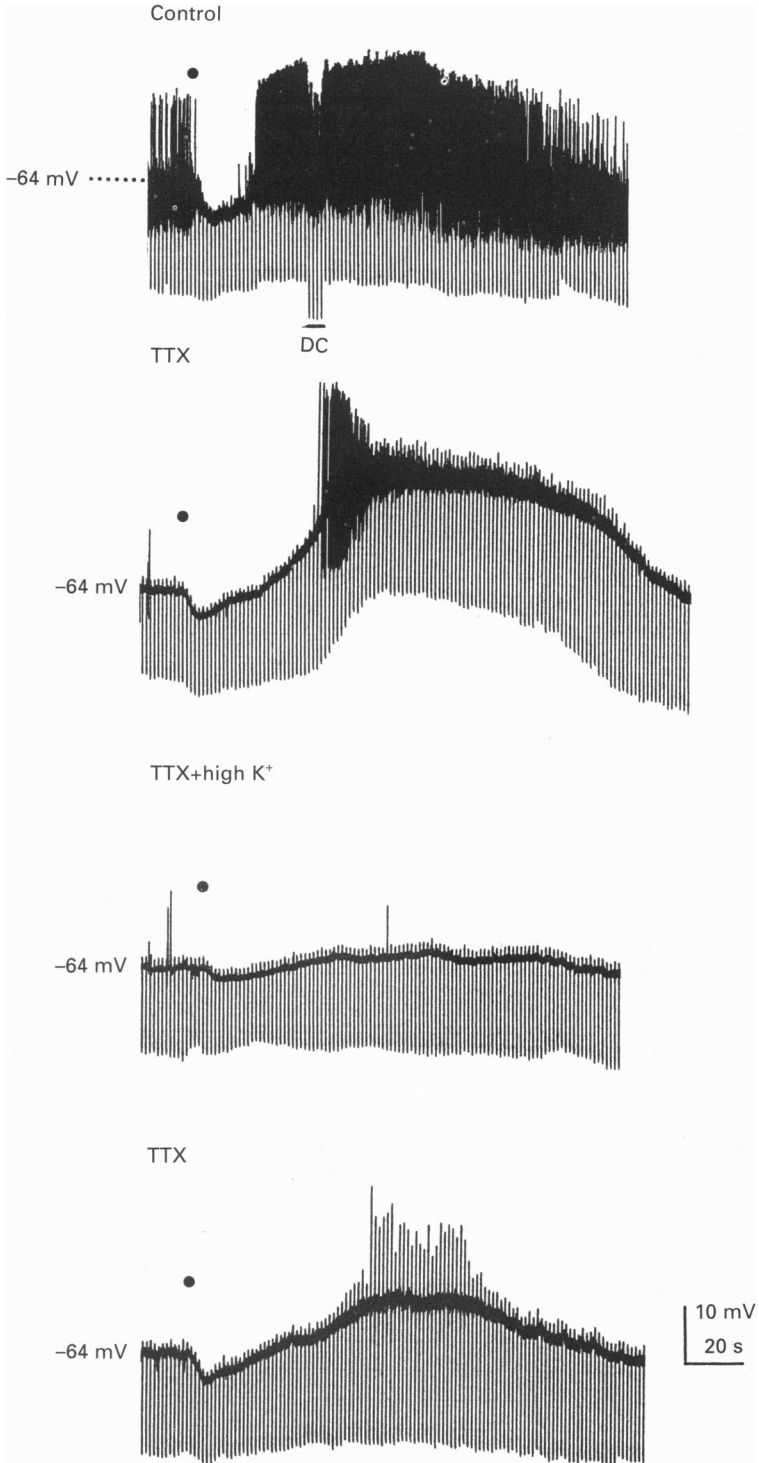
Fig. 7. For legend see facing page.

experiments. The possibility that a reduction in potassium conductance accounted for the slow cholinergic depolarizations in BLA pyramidal cells gained further support from the finding that carbachol-induced depolarizations could not be elicited in cells in which recordings were obtained with caesium acetate-filled electrodes (five of seven cases).

*Presynaptic versus postsynaptic nature of muscarinic hyperpolarizations and depolarizations*

To determine whether the responses produced by local application of carbachol were mediated by direct actions on BLA neurons, responses to brief pressure applications of drug were examined in twenty-five neurons under conditions where synaptic transmission was blocked. In all cases, superfusion of media containing TTX (1 $\mu$M, $n = 19$) or cadmium (100 $\mu$M, $n = 6$) totally abolished spontaneous postsynaptic potentials and synaptically evoked responses to EC stimulation but failed to block the depolarizing response to carbachol. In comparison, the initial hyperpolarizing component of the carbachol-induced response was greatly reduced ($n = 6$) or abolished ($n = 15$) when TTX or cadmium was present in the bath. The results from a typical experiment are shown in Fig. 8A. Note in this cell that the blockade of the hyperpolarization that occurred during bath superfusion of TTX was accompanied by a marked shortening of the onset latency of membrane depolarization to carbachol. This same phenomenon was observed in seven additional cells.

Recent evidence from our laboratory (Moises & Washburn, 1989), together with results from neurochemical and histochemical studies (McDonald, 1985; Nitecka & Ben-Ari, 1987, Nitecka & Frotscher, 1989) indicate that GABA-containing cells exert inhibitory synaptic control on pyramidal cells in the rat BLA. We therefore wondered whether the initial TTX- and cadmium-sensitive hyperpolarizing response to carbachol might be mediated indirectly through the activation of inhibitory interneurons which in turn produced IPSPs in the recorded cell. To test this hypothesis, neuronal responses to pressure application of carbachol were examined before and during superfusion of drugs known to block GABAergic neurotransmission. As shown in Fig. 8, in normal bathing medium, carbachol application produced an initial hyperpolarizing response followed by a depolarization (Fig. 8Ba, left panel), whereas electrical stimulation of amygdaloid afferents within the EC elicited a small EPSP followed by an early and late IPSP in the cell (Fig. 8Ba, right panel). When bicuculline methiodide (40 $\mu$M) was added to the bathing solution,

Fig. 7. Potassium dependence of the muscarinic depolarization. Chart records illustrate the membrane responses of a pyramidal cell to pressure application of oxotremorine-M (1 mM, 30 ms, ●) obtained in normal ACSF and in ACSF containing TTX with normal [K$^+$] (3·5 mM) or high [K$^+$] (7·0 mM). Administration of TTX reduced the initial hyperpolarization produced by pressure application of oxotremorine-M but did not affect the slow depolarization that was recorded in ACSF containing normal [K$^+$]$_o$. Note that the amplitude of the TTX-resistant depolarization was reversibly reduced when the external [K$^+$] was doubled. The large deflections seen during the depolarization in the TTX record represent Ca$^{2+}$ action potentials. Membrane potential was held to $-64$ mV with intracellular current injection prior to drug application. Resting membrane potential was $-72$ mV.
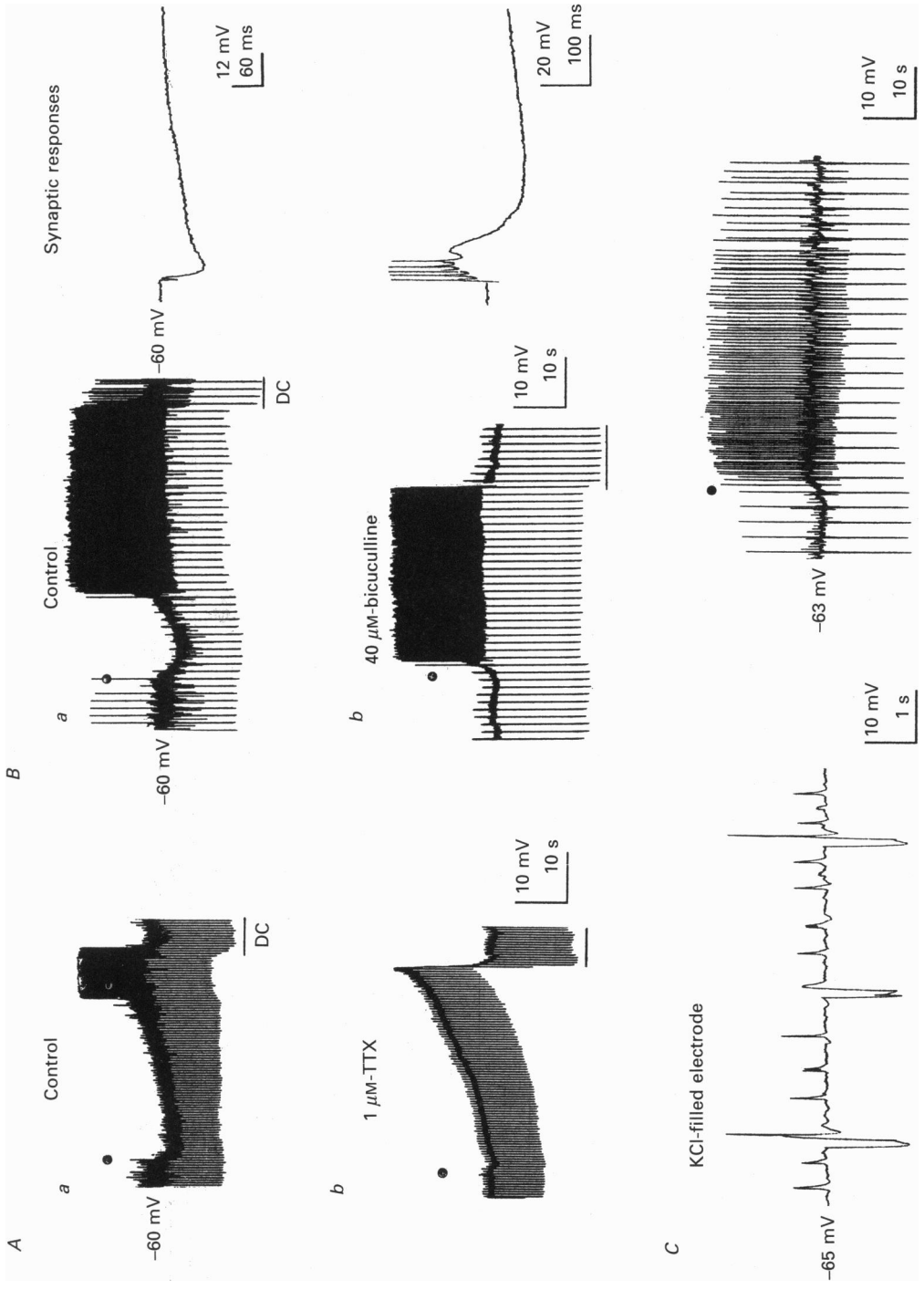
Fig. 8. For legend see facing page.

stimulation of the EC now elicited an epileptiform burst discharge followed by a prolonged hyperpolarization (Fig. 8*Bb*, right panel). Under these conditions, the initial hyperpolarizing response to carbachol was abolished and the onset latency of the carbachol-induced depolarization markedly decreased (Fig. 8*Bb*, left panel). Similar results were obtained during bath application of bicuculline (10–100 $\mu$M) in eight additional slices and an identical outcome was observed in six experiments in which the Cl$^-$ channel blocker picrotoxin (40 $\mu$M) was used to block GABA-mediated synaptic action in BLA (data not shown).

The preceding results strongly suggested that the hyperpolarizing response of BLA neurons to carbachol occurred indirectly via presynaptic release of GABA and the subsequent activation of GABA$_A$ receptors, leading to an increase in chloride conductance. If so, then these carbachol-induced hyperpolarizing responses should be sensitive to manipulations which alter the chloride gradient across the membrane. To shift the chloride gradient across the membrane, recordings were obtained with KCl-filled microelectrodes. When recording at resting membrane potential under these conditions, spontaneous IPSPs were seen as depolarizing rather than hyperpolarizing events (Fig. 8*C*, left) and brief applications of carbachol typically elicited only membrane depolarizations (Fig. 8*C*, right) rather than the biphasic responses recorded with potassium acetate-filled microelectrodes. Moreover, the reversal potential for the hyperpolarizing responses to carbachol that were recorded in neurons with KCl-filled electrodes was significantly more depolarized ($-67.3 \pm 1.3$ mV, $n = 8$) than for the response obtained with potassium acetate-filled electrodes ($-76.1 \pm 1.0$, $n = 25$, $P < 0.05$). No differences were noted between the carbachol-induced depolarizations recorded with KCl- *versus* potassium acetate-filled microelectrodes, suggesting that the increase in input resistance associated with muscarinic depolarizations was not due to a decrease in chloride conductance.

In the course of this study, recordings were obtained from ten BLA neurons whose electrophysiological properties were clearly distinct from those of pyramidal cells. These neurons had short-duration action potentials ($0.7 \pm 0.1$ ms, $n = 9$), a high rate of spontaneous or current-evoked discharge and showed no accommodation in response to intracellular current injection (Fig. 9*A*). These properties are virtually

---

Fig. 8. Mechanisms underlying membrane responses to pressure application of carbachol. *A*, the hyperpolarization elicited by carbachol pressure ejection (●) was abolished during bath perfusion of ACSF containing TTX, whereas the depolarization was unaffected. Note that the carbachol-induced depolarization was accompanied by a marked increase in input resistance, which was clearly revealed when the membrane potential was reset to the pre-drug level ($-60$ mV) by passage of direct current (DC). *Ba*, recordings obtained in normal medium illustrate the typical biphasic membrane response produced by pressure application of carbachol in another pyramidal cell. Digitized records at right show the synaptically evoked responses of this cell to EC stimulation that were recorded at a membrane potential of $-60$ mV. *Bb*, the hyperpolarizing response to carbachol was blocked by bicuculline methiodide while the amplitude of the depolarization was unaffected. Right, synaptic response recorded in bicuculline showing blockade of the early IPSP. *Ca*, expanded chart record of a recording obtained from a different neuron made with an electrode filled with 2 M-KCl. Note the spontaneous depolarizing IPSPs which are seen as the upward deflections above the baseline membrane potential. *Cb*, in the same cell, local application of carbachol (●) produced a short-latency depolarization without a preceding hyperpolarization. Resting membrane potentials were $-68$, $-71$ and $-65$ mV for the cells in *A*, *B* and *C*, respectively.

identical to those of intrinsic GABAergic interneurons in rat hippocampus (Lacaille & Schwartzkroin, 1988; Scharfman & Schwartzkroin, 1988) and cortex (Satou, Mori, Tazawa & Takagi, 1983; McCormick & Prince, 1986). Intracellular labelling of such BLA neurons with Lucifer Yellow showed them to have morphological features
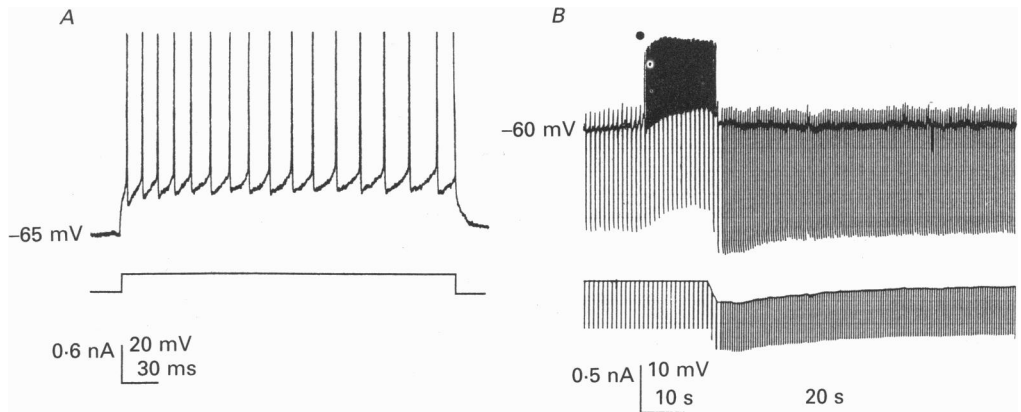


Fig. 9. Short-latency muscarinic depolarization of a presumptive BLA interneuron. *A*, membrane response elicited in this cell during intracellular injection of a 250 ms depolarizing pulse. Note absence of accommodation in spike discharge. *B*, response of the same cell to a brief (30 ms) pressure application of muscarine (1 mM, ●). Approximately 15 s after the onset of the muscarine-induced depolarization, the membrane potential of the cell was manually voltage clamped back to the pre-drug level. Inspection of the records at this time reveals that the depolarization was associated with an increase in input resistance as indicated by an increase in the size of the electrotonic potentials produced by passage of constant current hyperpolarizing pulses through the recording electrode. The lower traces in *A* and *B* correspond to the current records. Resting membrane potential was $-67$ mV.

which were distinct from pyramidal cells (see Washburn & Moises, 1990) and nearly identical to GABA-containing neurons that have been described in immuno-histochemical studies in rat BLA (McDonald, 1985; McDonald & Pearson, 1989). Pressure application of carbachol or muscarinic agonists to five presumptive interneurons resulted in an immediate membrane depolarization whose onset coincided with the initial inhibitory response recorded in pyramidal cells (Fig. 9*B*). The depolarization was associated with an increase in input resistance and was blocked by atropine ($n = 3$).

The preceding data suggest that in the large majority of cases an indirect mechanism accounted for the initial hyperpolarizing responses that were recorded in response to focal application of carbachol or muscarinic agonists. Nevertheless, it appeared that some of the hyperpolarizing responses to agonist application resulted from actions on the neuron under study since, in a few instances, they were not totally abolished by TTX (three of nineteen neurons tested, e.g. Fig. 7) or GABA antagonists (five of fifteen neurons). Interestingly, in these cases there was some indication that the hyperpolarization may have been mediated by an increase in potassium conductance, as evidenced by the relatively negative reversal potential of these responses ($-80{\cdot}6 \pm 1{\cdot}8$ mV, $n = 8$) and their sensitivity to changes in external
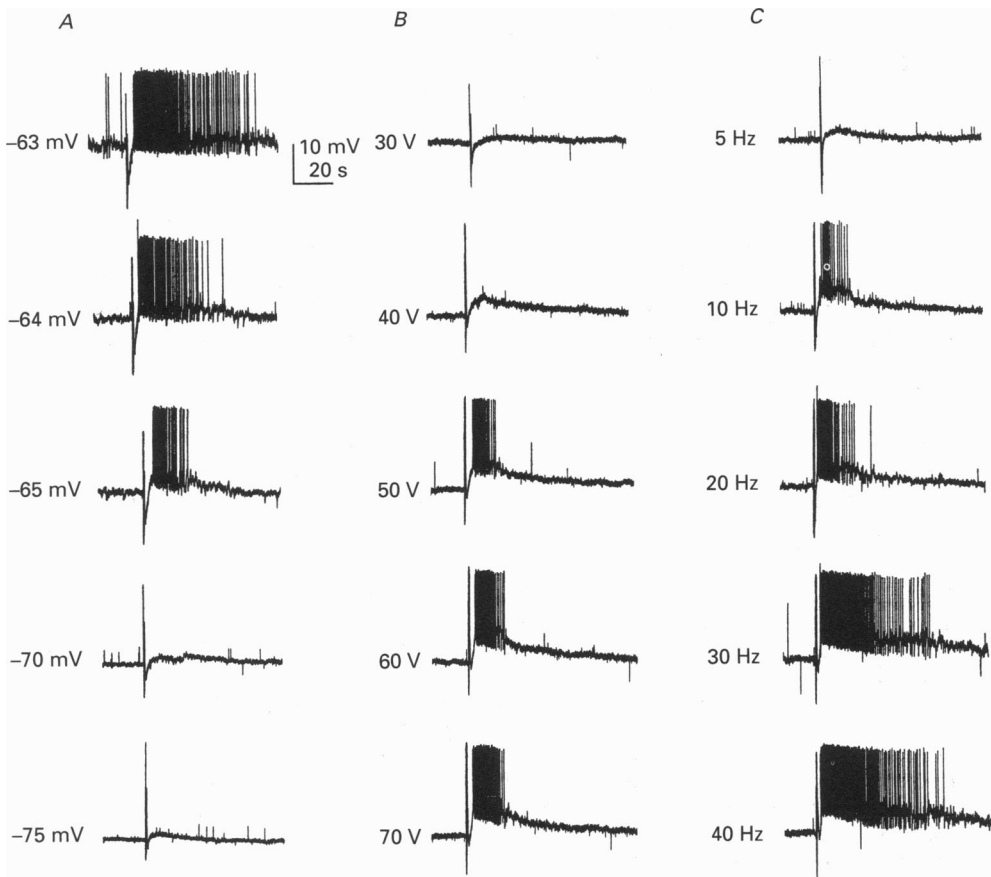
Fig. 10. Dependency of the amplitude of the cholinergic slow EPSP on membrane potential and parameters of cholinergic pathway stimulation. *A*, identical trains of electrical stimuli (500 ms, 30 Hz, 60 V) were delivered to the EC while the membrane potential was manually adjusted in the hyperpolarizing or depolarizing direction by injection of DC current through the recording electrode. *B*, the dependence of the slow EPSP amplitude on stimulus intensity was demonstrated by stimulating the EC with equal numbers of stimuli delivered at varying intensities. A 500 ms, 30 Hz train was utilized in this experiment. *C*, the dependence of the slow EPSP amplitude on stimulus frequency was demonstrated by stimulating the EC with stimulus trains (500 ms) of increasing frequency (top to bottom). The records in this figure were made from the same neuron during perfusion of medium containing 1 $\mu$M-eserine. Resting membrane potential was $-72$ mV.

potassium (Fig. 7). Since TTX-resistant muscarinic hyperpolarizations were relatively rare, we were unable to perform a more rigorous examination of the ionic mechanism underlying the response.

*Electrical stimulation of cholinergic fibres*

An important goal of this study was to compare the responses of BLA neurons to cholinomimetics with effects produced by synaptic release of ACh. By combining retrograde transport of fluorescently labelled markers with ChAT immuno-

histochemistry, Carlsen and colleagues (1985) showed that the source of cholinergic afferents to the BLA in rat originates from a continuum of cholinergic neurons extending from the ventral pallidum through the SI to ventral regions of the globus pallidus. Among these regions, it is the cholinergic neurons within the sublenticular SI that serve as the primary source of cholinergic input to the BLA (Nagai *et al.* 1982; Carlsen *et al.* 1985). The effects of electrical stimulation of these amygdalopetal cholinergic afferents were examined in recordings from forty-eight BLA pyramidal neurons in horizontal slices of rat forebrain which contained portions of the BLA and the SI. In recordings obtained in normal bathing media, repetitive stimulation of the SI typically at 30 Hz for 500 ms (with 0·1 ms stimuli) elicited a series of short-latency fast EPSPs or action potentials followed by a hyperpolarization (Figs 10 and 11). Repetitive stimulation of the EC, through which cholinergic afferents to the BLA have been shown to course (Ichikawa & Hirata, 1986), often elicited similar responses. The hyperpolarizing responses to tetanic stimulation of SI or EC were associated with a decrease in input resistance and had a reversal potential of $-73\cdot1\pm0\cdot9$ mV ($n = 13$), which is not significantly different ($P > 0\cdot05$) from that of the orthodromically evoked early IPSP ($-74\cdot9\pm1\cdot5$, $n = 15$) or the hyper-polarization produced by carbachol pressure ejection ($-76\cdot1\pm1\cdot0$ mV, $n = 25$). Superfusion of bicuculline methiodide (20 $\mu$M) greatly reduced the membrane hyperpolarization produced by repetitive stimulation of the SI ($n = 3$, data not shown). Taken together, these data suggest that the hyperpolarizing responses reflect the summed effect of repetitive activation of a $GABA_A$ receptor-mediated increase in chloride conductance.

In recordings obtained in normal bathing medium, a slow EPSP was seen to follow the hyperpolarizing response to SI or EC stimulation in six of the forty-eight cells studied when examined at resting membrane potential. Addition of the acetyl-cholinesterase inhibitor eserine (1–5 $\mu$M) to the bath increased the likelihood of evoking the slow EPSP. Thus, in the presence of eserine a slow EPSP was observed following the EC- or SI-induced hyperpolarization in thirty-three cells in which tetanic stimulation had failed to evoke slow depolarizing responses in normal medium. Eserine also increased the amplitude of the depolarizing response in those cases in which it was possible to elicit a slow EPSP in the absence of cholinesterase blockade. In the experiment shown in Fig. 11, for example, addition of eserine (2 $\mu$M) to the bath greatly increased the duration of the slow EPSP elicited by a 30 Hz stimulation of the SI. In this and other neurons, eserine itself (2–5 $\mu$M) had no effect on resting membrane potential or input resistance. The finding that the generation of the slow EPSP was blocked by atropine (Fig. 11*B*, right) (0·1–1 $\mu$M, $n = 15$) but not be hexamethonium (10–30 $\mu$M, $n = 3$) indicates that this response arose from the activation of muscarinic receptors.

To examine the properties of the slow EPSP, experiments were routinely carried out in the presence of eserine. Figure 10*A* shows the results of an experiment in which we examined the influence of membrane potential on the amplitude of the slow EPSP. In this pyramidal cell, and in nearly all other cells examined, the slow EPSP was small in amplitude when evoked at resting membrane potential (4·9±0·7 mV from an average resting membrane potential of $-68\cdot8\pm3\cdot1$ mV, $n = 28$). The slow EPSP, like the depolarizing response to exogenous application of cholinomimetics,
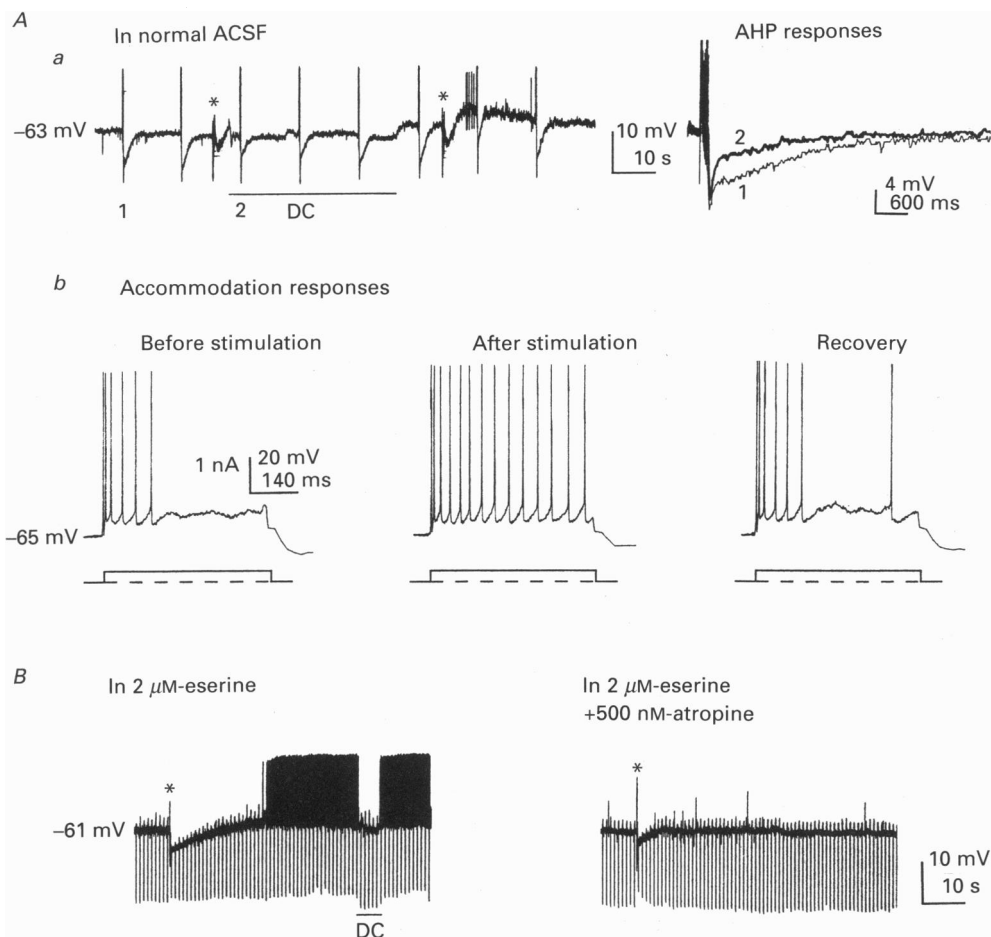
Fig. 11. Effect of activation of cholinergic amygdalopetal afferents on membrane potential, the AHP and spike frequency accommodation in a BLA pyramidal cell. *A a*, chart record (left) and computer-generated traces (right) show AHPs which followed a series of current-evoked actions potentials before (response marked by a '1') and after (response marked by '2') repetitive stimulation of the SI. Periods of SI stimulation are indicated by an asterisk above chart records. Immediately after delivery of the first cholinergic stimulation shown in the chart record, the membrane potential was manually voltage clamped to the pre-stimulus level to control for voltage-dependent changes in the evoked potentials (area marked DC in the trace). A second stimulation shown in the chart record reveals the slow EPSP without manual voltage clamp. *A b*, in the same cell, frequency accommodation was blocked for up to 30 s following repetitive stimulation of the SI. *B*, in the same cell, the initial hyperpolarizing response and subsequent slow EPSP evoked by repetitive stimulation of cholinergic afferents were enhanced in 2 $\mu$M-eserine (compare chart record in *B* to that in *A a*). The slow EPSP persisted from approximately 3 min beyond the point where the chart record was truncated. The facilitating effects of eserine on slow EPSP and the initial hyperpolarizing response were both blocked by atropine (500 nM) (right). Resting membrane potential was −72 mV.

showed a gradual reduction in size as the cell was hyperpolarized by intracellular injection of constant current. Conversely, when responses were elicited as the cell was depolarized to near firing threshold, the size of the slow EPSP increased and responses were often associated with a prolonged period (1–4 min) of intense firing. In most cases, the slow EPSP could not be elicited below a membrane potential of $-75$ mV ($E_{rev} = -72 \cdot 8 \pm 3 \cdot 1$ mV, $n = 15$). Measurements made in ten cells revealed that the slow EPSP was associated with an increase in membrane input resistance of $14 \cdot 7 \pm 2 \cdot 3\%$, when elicited at $-65$ mV. This can clearly be seen in Fig. 11$B$ (left) by comparing the amplitude of membrane potential deflections caused by constant current hyperpolarizing pulses delivered during the slow EPSP at a time when the membrane potential was returned to the baseline level by passage of a steady hyperpolarizing current (DC).

The size of the slow EPSP was shown to be graded directly in relation to both the intensity and the number of stimuli used to activate cholinergic afferents within the slice. In the records shown in Fig. 10$B$ and $C$, slow EPSPs were recorded with the cell held at a constant depolarized level while systematically varying the stimulus intensity or frequency of electrical stimulation delivered to the SI. While single stimuli could sometimes elicit a slow EPSP in the presence of eserine, the responses showed marked summation as the frequency of stimulation was increased and approached a maximum at approximately 40–50 Hz. Similar results were obtained in experiments on eight other BLA neurons.

The generation of muscarinic slow EPSPs in the rat hippocampal slice preparation has previously been shown to be dependent on propagated action potentials (Cole & Nicoll, 1984). Although the distance between the stimulating and recording electrodes in this study was usually at least 3 mm, the possibility exists that the slow EPSP was generated by ACh release arising from direct current spread through the slice. However, our inability to elicit slow EPSPs in the presence of TTX (1 $\mu$M, $n = 4$) or cadmium (100 $\mu$M, $n = 4$) argues against this explanation and indicates that these muscarinic responses were dependent on the propagation of action potentials and were mediated by a calcium-dependent process.

In the final series of experiments we sought to determine whether synaptic release of ACh resulted in a blockade of spike frequency accommodation and a reduction in the slow AHP that follows a current-evoked burst of spikes in BLA pyramidal cells. Figure 11$Aa$ shows the results of an experiment performed in normal bathing medium in which a cholinergic slow EPSP was elicited in a BLA neuron by repetitive stimulation of SI. Under these conditions, a marked but transient reduction in the size of the slow AHP (downward deflections in voltage trace) was produced following 30 Hz stimulation of the SI for 500 ms. This can be seen by comparing the slow component of the AHP generated before SI stimulation (response marked by '1') to that recorded during the peak of the stimulus-evoked slow EPSP, at a time when the membrane potential was manually voltage-clamped to the pre-stimulus level (response marked by '2'). In the same pyramidal cell, repetitive stimulation of the SI was also effective in blocking spike frequency accommodation (Fig. 11$B$). It should be noted that these effects were commonly observed independent of the generation of the synaptically evoked slow depolarization. The depressant effects of cholinergic pathway stimulation on the AHP and spike frequency accommodation

were blocked by atropine (1 $\mu$M, $n = 12$) and pirenzepine (300 nM–1 $\mu$M, $n = 7$), but not by hexamethonium (10–30 $\mu$M, $n = 3$). In the majority of cells studied, administration of eserine alone (2–5 $\mu$M) in the absence of cholinergic pathway stimulation reduced the slow AHP and blocked accommodation in an atropine-sensitive manner (0·5–1 $\mu$M, $n = 8$). These latter findings indicate the presence of a substantial tonic release of endogenous ACh in the slice.

<center>DISCUSSION</center>

The present study has provided the first description of cholinergic effects on neurons in the rat BLA. In our experiments we compared the actions of carbachol and other cholinomimetics on BLA pyramidal neurons to the responses evoked by stimulation of endogenous ACh release in the slice. The cholinergic effects described here were remarkably similar to muscarinic actions that have been found in pyramidal neurons in slice preparations of rat and guinea-pig hippocampus (Cole & Nicoll, 1984; Madison *et al.* 1987; Segal, 1988; Dutar & Nicoll, 1988; Misgeld, Muller & Polder, 1989) and cortex (McCormick & Prince, 1986; Constanti & Sim, 1987). All of the cholinergic effects that we have observed in BLA pyramidal neurons were blocked by muscarinic, but not nicotinic antagonists, indicating their mediation via muscarinic receptors.

*Muscarinic depolarization*

The activation of muscarinic receptors by carbachol or muscarinic agonists often resulted in membrane depolarizations and induced repetitive firing. These depolarizations were associated with an increase in input resistance and were voltage dependent in that, in many cases, the depolarizations were evoked only when the cell under study was depolarized to near firing threshold prior to drug application. Slow muscarinic cholinergic depolarizations having properties similar to those in BLA pyramidal cells have also been observed in a variety of other neurons in both the central and peripheral nervous systems (for review see North, 1989). In the vast majority of cases, the increase in input resistance and resultant depolarization have been attributed either to the blockade of a potassium leak conductance which contributes to resting membrane potential ($I_{K,leak}$) (Dodd, Dingledine & Kelly, 1981; Benardo & Prince, 1982; Morita, North & Tokimasa, 1982; Madison *et al.* 1987; Benson *et al.* 1988; Greene, Gerber & McCarley, 1989; Pitler & Alger, 1990) or to a reduction in the time- and voltage-dependent conductance, $I_M$ (Adams & Brown, 1982; Benardo & Prince, 1982; Halliwell & Adams, 1982). The muscarinic depolarization observed in BLA pyramidal neurons also appeared to be mediated by a reduction in potassium conductance since it was associated with an increase in membrane input resistance, was sensitive to changes in the extracellular potassium concentration and was typically not observed in cells in which recordings were made with caesium acetate-filled microelectrodes. Furthermore, the finding of voltage-sensitive and voltage-insensitive muscarinic depolarizations is compatible with the suggestion that reductions of $I_M$ and $I_{K,leak}$, respectively, might account for the slow muscarinic depolarization in BLA pyramidal neurons. More direct evidence supporting this hypothesis derives from recent voltage-clamp experiments in our

laboratory which indicate that both of these currents serve as targets of inhibitory muscarinic actions in BLA pyramidal cells (Womble & Moises, 1990). In those experiments, bath application of carbachol was found to block $I_M$ directly and also produced an inward shift in holding current when neurons were voltage clamped to negative potentials (beyond $-65$ mV) where $I_M$ is inactivated. Similar voltage-clamp results have been reported in rat hippocampal pyramidal cells (Madison *et al.* 1987; Benson *et al.* 1988).

*Muscarinic blockade of calcium-dependent potassium conductance*

The slow AHP recorded in BLA pyramidal cells following a current-evoked burst of action potentials has previously been shown to be reduced by cadmium and noradrenaline (Gean & Shinnick-Gallagher, 1989). In the experiments reported here, the slow AHP was blocked by caesium, EGTA or 8-bromo-cyclic AMP, providing further evident that it is mediated by a calcium-activated potassium conductance. Carbachol or muscarinic agonists markedly reduced the slow AHP and concomitantly blocked spike frequency accommodation. Similar actions have been described in neurons in rat hippocampus (Cole & Nicoll, 1986; Muller & Misgeld, 1986; Lancaster & Nicoll, 1987; Madison *et al.* 1987; Dutar & Nicoll, 1988) and cortex (McCormick & Prince, 1986; Constanti & Sim, 1987), guinea-pig sympathetic ganglia (Cassell & McLachlan, 1987) and guinea-pig myenteric plexus (North & Tokimasa, 1983; Galligan, North & Tokimasa, 1989). In the present study, calcium spikes were unaffected during carbachol superfusion at the same time that slow AHPs were diminished. An identical result in hippocampal pyramidal cells (Cole & Nicoll, 1984) was taken to indicate that the muscarinic reduction of the slow AHP occurred at some step subsequent to calcium entering the cell, possibly via a direct inhibitory action on the underlying conductance. In support of this view, by combining intracellular recordings with microfluorometric recording techniques Knopfel and co-workers (1990) were able to demonstrate that the inhibition of $I_{AHP}$ by muscarine is not mediated by alterations in calcium dynamics in hippocampal pyramidal cells. Nevertheless, it should be noted that muscarinic reduction of calcium currents has been reported in both the CNS (striatal neurons: Misgeld, Calabresi & Dodt, 1986; cultured hippocampal cells; Gahwiler & Brown, 1987) and in the periphery (myenteric neurons; North & Tokimasa, 1983; sympathetic ganglion cells: Belluzzi, Sacchi & Wanke, 1985; Wanke, Ferroni, Malgaroli, Ambrosini, Pozzan & Meldolesi, 1987).

The most parsimonious explanation for the muscarinic blockade of spike frequency accommodation is that it also results from a blockade of the calcium-dependent potassium conductance. However, it is conceivable that a reduction in $I_M$ could contribute to the block of accommodation, as has been suggested in hippocampal pyramidal cells (Madison & Nicoll, 1984) and bull-frog sympathetic neurons (Adams, Brown & Constanti, 1982). While the current-clamp experiments described here do not allow one to assess muscarinic actions on currents directly, preliminary results from a recent voltage-clamp study showed only small reductions in $I_M$ at concentrations of carbachol which block accommodation in BLA neurons (Womble & Moises, 1990). This latter study also demonstrated that carbachol does not reduce $I_A$, a transient potassium current which is also involved in spike frequency accommodation in these cells (Gean & Shinnick-Gallagher, 1989).

*Muscarinic reduction of synaptic responses*

Superfusion of carbachol or muscarinic agonists was found to decrease the amplitude of the EPSPs evoked in BLA pyramidal cells following EC stimulation. Similar muscarinic reductions of synaptically evoked EPSPs have been described elsewhere in the CNS (Hounsgaard, 1978; Valentino & Dingledine, 1981; Dodt & Misgeld, 1985) and pharmacological analyses indicate that such effects appear to be mediated presynaptically via an $M_2$-type receptor (North, Slack & Surprenant, 1985; Dutar & Nicoll, 1988). Synaptically evoked IPSPs have also been shown to be reduced by muscarinic receptor activation in the rat hippocampus (Ben-Ari, Krnjevic, Reinhardt & Roper, 1981; Haas, 1982), rat dorsolateral septal nucleus (Hasuo, Gallagher & Shinnick-Gallagher, 1988) and guinea-pig submucosal plexus (North *et al*. 1985). At a time when carbachol reduced spontaneous and stimulus-evoked IPSPs in BLA pyramidal cells, postsynaptic responses of BLA neurons to GABA or baclofen were unaffected. These findings suggest that the cholinergic reduction of inhibitory synaptic events seen here results from a presynaptic inhibition of GABA release rather than alterations in postsynaptic chemosensitivity. The anatomical substrate for such a mechanism was suggested by recent immunohistochemical studies which revealed ChAT-immunoreactive nerve terminals in close apposition to synapses between presumed GABAergic terminals and somata of pyramidal cells in the BLA (Carlsen, 1988, 1989; Nitecka & Frotscher, 1989).

*Mechanism underlying muscarinic inhibition*

Several lines of evidence indicate that, with few exceptions, the initial short-latency hyperpolarizing responses of BLA pyramidal cells to pressure application of carbachol were mediated indirectly via a GABA-mediated increase in chloride conductance. First, these inhibitory responses were largely abolished by superfusion of TTX (1 $\mu$M) or cadmium (100 $\mu$M). Second, the hyperpolarizing response was markedly reduced or eliminated during superfusion of GABA antagonists. Third, the reversal potential of the carbachol-induced hyperpolarization was identical to that of the $GABA_A/Cl^-$-mediated early IPSP and it shifted in the depolarizing direction when the $Cl^-$ gradient across the membrane was reduced. Finally, in recordings obtained from a limited number of presumptive GABAergic interneurons in the BLA, pressure application of carbachol or muscarinic agonists was found to produce a short-latency excitatory response whose onset coincided with that of the hyperpolarization recorded in BLA pyramidal neurons. The anatomical basis for cholinergic actions on inhibitory interneurons in the BLA was provided by a double immunolabelling study in the rat amygdala which showed that ChAT-im-munoreactive nerve terminals form synaptic contacts on somata and dendrites of neurons containing the synthetic enzyme for GABA (Nitecka & Frotscher, 1989).

*Muscarinic slow EPSP*

Stimulation of cholinergic afferents to the BLA evoked postsynaptic responses that exactly mimicked the actions produced by administration of carbachol or muscarinic agonists. Thus, repetitive stimulation of the SI or EC elicited a slow muscarinic EPSP associated with an increase in membrane input resistance. Like the muscarinic slow depolarization that was produced by pressure application of

cholinomimetics, the slow EPSP was sensitive to changes in membrane potential, being reduced in amplitude with membrane hyperpolarization.

It is of interest to compare the cholinergic slow EPSP found in BLA neurons to muscarinic depolarizing synaptic potentials recorded in neurons in the peripheral nervous system (North & Tokimasa, 1984; Brown & Selyanko, 1985*a*, *b*) and in a number of brain areas (Cole & Nicoll, 1984; Dodt & Misgeld, 1986; Madison *et al.* 1987; Segal, 1988; Misgeld *et al.* 1989). While we did not characterize the ionic mechanism underlying the slow EPSP, its overall similarity to many of the carbachol-induced depolarizations suggested that it resulted mainly from a muscarinic reduction of a resting potassium leak conductance which was not strongly voltage dependent. This same conclusion has been reached in current- and voltage-clamp experiments carried out in pyramidal cells of the CA1 (Madison *et al.* 1987) and CA3 (Misgeld *et al.* 1989) regions of rat and guinea-pig hippocampus, in neurons in rat neostriatum (Dodt & Misgeld, 1986) and myenteric plexus neurons (Morita *et al.* 1982). None the less, studies by other investigators suggest that a reduction in $I_M$ primarily accounts for slow EPSPs that are produced following stimulation of cholinergic afferents in some of these same neurons (Cole & Nicoll, 1984; Brown & Selyanko, 1985*a*, *b*; Gahwiler & Brown, 1987). We cannot rule out the possibility that a reduction in the $I_M$ contributes to the slow EPSP in this study, especially in experiments where the response was steeply voltage dependent and could only be elicited in the range where this current is thought to be active. However, we can be reasonably certain that a blockade of the calcium-dependent potassium conductance underlying the slow AHP does not contribute significantly to the depolarization since the slow EPSP persisted in conditions such as 8-bromo-cyclic AMP in which the slow AHP and accommodation were abolished. This conclusion is supported by previous investigations in rat hippocampus (Gahwiler & Brown, 1985; Madison *et al.* 1987).

The second major muscarinic effect produced by repetitive stimulation of the SI or EC was a reduction in the slow AHP that follows a burst of action potentials and the concomitant block of spike frequency accommodation. The finding that the cholinergic reduction in the AHP and accommodation produced by repetitive stimulation could occur independent of changes in membrane potential suggests that $I_{AHP}$ is more sensitive to blockade by ACh than is the conductance or conductances which underlies the slow EPSP. This finding also indicates that in BLA pyramidal cells, as in hippocampal pyramidal cells (Cole & Nicoll, 1984; Segal, 1988), $I_{AHP}$ does not contribute to resting membrane potential. Bath application of eserine alone, in the absence of afferent stimulation, reduced both the AHP and accommodation. This suggests that there is a tonic release of ACh, but that the activity of acetyl-cholinesterase in the slice is sufficiently high to prevent postsynaptic effects of the tonically released ACh.

In summary, the results of the experiments described here have demonstrated a number of mechanisms whereby cholinergic input can affect the excitability of BLA neurons. It appears that blockade of at least three potassium conductances, $I_M$, $I_{AHP}$ and $I_{K,leak}$, may underlie direct muscarinic excitatory actions on BLA pyramidal cells. The overall contribution of these conductances under normal conditions appears to stabilize the membrane potential and to serve as a braking mechanism in

controlling the repetitive discharge pattern of the cell (Brown, 1983). Thus, the net outcome of muscarinic suppression of these currents may include membrane depolarizations and a general increase in the neuronal output frequency to prolonged excitatory inputs. The finding here that muscarinic cholinergic blockade of $I_{AHP}$ occurred in the absence of membrane depolarizations suggests that the major influence of activation of cholinergic input to the BLA may be to regulate the postsynaptic responsiveness of target neurons to conventional excitatory afferent input rather than to modulate their inherent pattern of spike generation. The muscarinic reduction of inhibitory synaptic responses suggests an additional mechanism whereby the overall excitability of BLA neurons might be increased under conditions of increased cholinergic afferent activity. Further examination of the cholinergic regulations of BLA neuronal excitability clearly seems warranted in light of the well-recognized importance of this brain region in the generation of epileptiform activity (Gloor, Olivier, Quesney, Andermann & Horowitz, 1982) and of emerging evidence of its role in memory function (for review see Sarter & Markowitsch, 1985).

## REFERENCES

ADAMS, P. R. & BROWN, D. A. (1982). Synaptic inhibition of the M-current: slow excitatory post-synaptic potential mechanism in bullfrog sympathetic neurones. *Journal of Physiology* **332**, 263–272.

ADAMS, P. R., BROWN, D. A. & CONSTANTI, A. (1982). Pharmacological inhibition of the M-current. *Journal of Physiology* **332**, 223–262.

BELLUZZI, O., SACCHI, O. & WANKE, E. (1985). Identification of delayed potassium and calcium currents in the rat sympathetic neurone under voltage clamp. *Journal of Physiology* **358**, 109–129.

BEN-ARI, Y., KRNJEVIC, K., REINHARDT, W. & ROPERT, N. (1981). Intracellular observations on the disinhibitory action of acetylcholine in the hippocampus. *Neuroscience* **6**, 2475–2484.

BEN-ARI, Y., ZIGMOND, R. E., SHUTE, C. C. D. & LEWIS, P. R. (1977). Regional distribution of choline acetyltransferase and acetylcholinesterase within the amygdaloid complex and stria terminalis system. *Brain Research* **120**, 435–445.

BENARDO, L. S. & PRINCE, D. A. (1982). Cholinergic excitation of mammalian hippocampal pyramidal cells. *Brain Research* **249**, 315–331.

BENSON, D. M., BLITZER, R. D. & LANDAU, E. M. (1988). An analysis of the depolarization produced in guinea-pig hippocampus by cholinergic receptor stimulation. *Journal of Physiology* **404**, 479–496.

BROWN, D. A. (1983). Slow cholinergic excitation – a mechanism for increasing neuronal excitability. *Trends in Neurosciences* **10**, 302–307.

BROWN, D. A. & SELYANKO, A. A. (1985a). Two components of muscarine-sensitive membrane current in rat sympathetic neurones. *Journal of Physiology* **358**, 335–363.

BROWN, D. A. & SELYANKO, A. A. (1985b). Membrane currents underlying the cholinergic slow excitatory postsynaptic potential in the rat sympathetic ganglion. *Journal of Physiology* **365**, 365–387.

CARLSEN, J. (1988). Immunocytochemical localization of glutamate decarboxylase in the rat basolateral amygdaloid nucleus, with special reference to GABAergic innervation of amygdalostriatal projection neurones. *Journal of Comparative Neurology* **273**, 513–526.

CARLSEN, J. (1989). New perspectives on the functional anatomical organization of the basolateral amygdala. *Acta Neurologica Scandinavica Supplementum* **122**, 1–27.

CARLSEN, J. & HEIMER, L. (1988). The basolateral amygdaloid complex as a cortical-like structure. *Brain Research* **441**, 377–380.

CARLSEN, J., ZABORSZKY, L. & HEIMER, L. (1985). Cholinergic projections from the basal forebrain to the basolateral amygdaloid complex: a combined retrograde fluorescent and immuno-histochemical study. *Journal of Comparative Neurology* **234**, 155–167.

CARLSEN, J. & HEIMER, L. (1986). A correlated light and electron microscopic immunocytochemical study of cholinergic terminals and neurones in the rat amygdaloid body with special emphasis on the basolateral amygdaloid nucleus. *Journal of Comparative Neurology* **244**, 121–136.

CASSELL, J. F. & MCLACHLAN, E. M. (1987). Muscarinic agonists block five different potassium conductances in guinea-pig sympathetic neurones. *British Journal of Pharmacology* **91**, 259–261.

COLE, A. E. & NICOLL, R. A. (1984). Characterization of a slow cholinergic post-synaptic potential recorded *in vitro* from rat hippocampal pyramidal cells. *Journal of Physiology* **352**, 173–188.

CONSTANTI, A. & SIM, J. A. (1987). Calcium-dependent potassium conductance in guinea-pig olfactory cortex neurones *in vitro*. *Journal of Physiology* **287**, 173–194.

DODD, J., DINGLEDINE, R. & KELLY, J. S. (1981). The excitatory action of acetylcholine on hippocampal neurones of the guinea pig and rat maintained *in vitro*. *Brain Research* **207**, 109–127.

DODT, H. U. & MISGELD, U. (1986). Muscarinic slow excitation and muscarinic inhibition of synaptic transmission in the rat neostriatum. *Journal of Physiology* **280**, 593–608.

DUTAR, P. & NICOLL, R. A. (1988). Classification of muscarinic responses in hippocampus in terms of receptor subtypes and second-messenger systems: electrophysiological studies *in vitro*. *Journal of Neuroscience* **8**, 4214–4224.

EMSON, P. C., PAXINOS, G., LE GAL LA SALLE, G., BEN-ARI, Y. & SILVER, A. (1979). Choline acetyltransferase and acetylcholinesterase containing projections from the basal forebrain to the amygdaloid complex of the rat. *Brain Research* **165**, 271–282.

GAHWILER, B. H. & BROWN, D. A. (1987). Muscarine affects calcium-currents in rat hippocampal pyramidal cells *in vitro*. *Neuroscience Letters* **76**, 301–306.

GALLIGAN, J. J., NORTH, R. A. & TOKIMASA, (1989). Muscarinic agonists and potassium currents in guinea-pig myenteric neurones. *British Journal of Pharmacology* **96**, 193–203.

GEAN, P. W. & SHINNICK-GALLAGHER, P. (1989). The transient potassium current, the A-current, is involved in spike frequency adaptation in rat amygdala neurones. *Brain Research* **480**, 160–169.

GLOOR, P., OLIVIER, A., QUESNEY, L. F., ANDERMANN, F. & HOROWITZ, S. (1982). The role of the limbic system in experiential phenomena of temporal lobe epilepsy. *Annals of Neurology* **12**, 129–144.

GREENE, R. W., GERBER, U. & MCCARLEY, R. W. (1989). Cholinergic activation of medial pontine reticular formation neurones *in vitro*. *Brain Research* **476**, 154–159.

HAAS, H. L. (1982). Cholinergic disinhibition in hippocampal slices of the rat. *Brain Research* **233**, 200–204.

HALLIWELL, J. V. & ADAMS, P. R. (1982). Voltage-clamp analysis of muscarinic excitation in hippocampal neurones. *Brain Research* **250**, 71–92.

HASUO, H., GALLAGHER, J. P. & SHINNICK-GALLAGHER, P. (1988). Disinhibition in the rat septum mediated by $M_1$ muscarinic receptors. *Brain Research* **438**, 323–327.

HELLENDALL, R.P., GODFREY, D. A., ROSS, C. D., ARMSTRONG, D. M. & PRICE, J. L. (1986). The distribution of choline acetyltransferase in the rat amygdaloid complex and adjacent cortical areas, as determined by quantitative micro-assay and immunohistochemistry. *Journal of Comparative Neurology* **249**, 486–498.

HOUNSGAARD, J. (1978). Presynaptic inhibitory action of acetylcholine in area CA1 of the hippocampus. *Experimental Neurology* **62**, 787–797.

ICHIKAWA, T. & HIRATA, Y. (1986). Organization of choline acetyltransferase-containing structures in the forebrain of the rat. *Journal of Neuroscience* **6**, 291–292.

KNÖPFEL, T., VRANESIC, I., GÄHWILER, B. H. & BROWN, D. A. (1990). Muscarinic and $\beta$-adrenergic depression of the slow $Ca^{2+}$-activated potassium conductance in hippocampal CA3 pyramidal cells is not mediated by a reduction of depolarization-induced cytosolic $Ca^{2+}$ transients. *Proceedings of the National Academy of Sciences of the USA* **87**, 4083–4087.

LACAILLE, J. C. & SCHWARTZKROIN, P. A. (1988). Stratum lacunosum-moleculare interneurones of hippocampal CA1 region I. Intracellular response characteristics, synaptic responses, and morphology. *Journal of Neuroscience* **8**, 1400–1410.

LANCASTER, B. & NICOLL, R. A. (1987). Properties of two calcium-activated hyperpolarizations in rat hippocampal neurones. *Journal of Physiology* **389**, 187–203.

LEWIS, P. R. & SHUTE, C. C. (1967). The cholinergic limbic system: projections to hippocampal formation medial cortex, nuclei of the ascending cholinergic reticular system and the subformal organ and supra-optic crest. *Brain* **90**, 521–540.

McCORMICK, D. A. & PRINCE, D. A. (1986). Mechanisms of action of acetylcholine in the guinea-pig cerebral cortex *in vitro*. *Journal of Physiology* **375**, 169–194.

MCDONALD, A. J. (1982). Neurones of the lateral and basolateral amygdaloid nuclei: a Golgi study in the rat. *Journal of Comparative Neurology* **212**, 293–312.

McDONALD, A. J. (1984). Neuronal organization of the lateral and basolateral amygdaloid nuclei in the rat. *Journal of Comparative Neurology* **222**, 589–606.

McDONALD, A. J. (1985). Immunohistochemical identification of gamma-aminobutyric acid-containing neurones in the rat basolateral amygdala. *Neuroscience Letters* **53**, 203–207.

McDONALD, A. J. & PEARSON, J. C. (1989). Coexistence of GABA and peptide immunoreactivity in non-pyramidal neurones of the basolateral amygdala. *Neuroscience Letters* **100**, 53–58.

MADISON, D. V. & NICOLL, R. A. (1984). Control of repetitive discharge of rat CA1 pyramidal neurones *in vitro*. *Journal of Physiology* **354**, 319–331.

MADISON, D. V., LANCASTER, B. & NICOLL, R. A. (1987). Voltage clamp analysis of cholinergic action in the hippocampus. *Journal of Neuroscience* **7**, 733–741.

MESULAM, M. M., MUFSON, E. J., LEVEY, A. I. & WAINER, B. H. (1983). Cholinergic innervation of cortex by the basal forebrain: cytochemistry and cortical connections of the septal area, diagonal band nuclei, nucleus basalis (substantia innominata), and hypothalamus in the rhesus monkey. *Journal of Comparative Neurology* **214**, 170–197.

MILLHOUSE, O. E. & DEOLMOS, J. (1983). Neuronal configurations in lateral and basolateral amygdala. *Neuroscience* **10**, 1269–1300.

MISGELD, U., CALABRESI, P. & DODT, H. U. (1986). Muscarinic modulation of calcium-dependent plateau potentials in rat neostriatal neurones. *Pflügers Archiv* **407**, 482–487.

MISGELD, U., MULLER, W. & POLDER, H. R. (1989). Potentiation and suppression by eserine of muscarinic synaptic transmission in the guinea-pig hippocampal slice. *Journal of Physiology* **409**, 191–206.

MOISES, H. C. & WASHBURN, M. S. (1989). Pharmacology of inhibitory responses recorded in basolateral and lateral amygdaloid neurones *in vitro*. *Society for Neuroscience Abstracts* **15**, 525.

MORITA, K., NORTH, R. A. & TOKIMASA, T. (1982). Muscarinic presynaptic inhibition of synaptic transmission in myenteric plexus of guinea-pig ileum. *Journal of Physiology* **333**, 141–149.

MULLER, W. & MISGELD, U. (1986). Slow cholinergic excitation of guinea-pig hippocampal neurones is mediated by two muscarinic receptor subtypes. *Neuroscience Letters* **67**, 107–112.

NAGAI, T., KIMURA, H., MAEDA, T., McGEER, P. L., PENG, F. & McGEER, E. G. (1982). Cholinergic projections from the basal forebrain of rat to the amygdala. *Journal of Neuroscience* **2**, 513–520.

NITECKA, L. & BEN-ARI, Y. (1987). Distribution of GABA-like immunoreactivity in the rat amygdaloid complex. *Journal of Comparative Neurology* **266**, 45–55.

NITECKA, L. & FROTSCHER, M. (1989). Organization and synaptic interconnections of GABAergic and cholinergic elements in the rat amygdaloid nuclei: single- and double-immunolabelling studies. *Journal of Comparative Neurology* **279**, 470–488.

NORTH, R. A. (1989). Muscarinic cholinergic receptor regulation of ion channels. In *The Muscarinic Receptors*, ed. BROWN, J. H., pp. 341–373. Humana Press, Clifton, NJ, USA.

NORTH, R A., SLACK, B. E. & SURPRENANT, A. (1985). Muscarinic $M_1$ and $M_2$ receptors mediate depolorization and presynaptic inhibition in guinea-pig myenteric nervous system. *Journal of Physiology* **368**, 435–452.

NORTH, R. A. & TOKIMASA, T. (1983). Depression of calcium-dependent potassium conductance of guinea-pig myenteric neurones by muscarinic agonists. *Journal of Physiology* **342**, 253–266.

NORTH, R. A. & TOKIMASA, T. (1984). The time course of muscarinic depolarization of guinea-pig myenteric neurones. *British Journal of Pharmacology* **82**, 85–91.

PAXINOS, G. & WATSON, C. (1986). *The Rat Brain in Stereotaxic Coordinates*. Academic Press, Sydney.

PITLER, T. A. & ALGER, B. E. (1990). Activation of the pharmacologically defined $M_3$ muscarinic receptor depolarizes hippocampal pyramidal cells. *Brain Research* **534**, 257–262.

SARTER, M. & MARKOWITSCH, H. J. (1985). The amygdala's role in human mnemonic processing. *Cortex* **21**, 7–24.

SATOU, M., MORI, K., TAZAWA, Y. & TAKAGI, S. F. (1983). Interneurones mediating fast postsynaptic inhibition in pyriform cortex of the rabbit. *Journal of Neurophysiology* **50**, 89–101.

SCHARFMAN, H. E. & SCHWARTZKROIN, P. A. (1988). Electrophysiology of morphologically identified mossy cells of the dentate hilus recorded in guinea pig hippocampal slices. *Journal of Neuroscience* **8**, 3812–3821.

SEGAL, M. (1988). Synaptic activation of a cholinergic receptor in rat hippocampus. *Brain Research* **452**, 79–86.

STORM, J. F. (1989). An after-hyperpolarization of medium duration in rat hippocampal pyramidal cells. *Journal of Physiology* **409**, 171–190.

VALENTINO, R. J. & DINGLEDINE, R. (1981). Presynaptic inhibitory effect of acetylcholine in the hippocampus. *Journal of Neuroscience* **1**, 784–792.

WANKE, E., FERRONI, A., MALGAROLI, A., AMBROSINI, A., POZZAN, T. & MELDOLESI, J. (1987). Activation of muscarinic receptor selectively inhibits a rapidly inactivated $Ca^{2+}$ current in rat sympathetic neurones. *Proceedings of the National Academy of Sciences of the USA* **84**, 4313–4317.

WASHBURN, M. S. & MOISES, H. C. (1989). Muscarinic responses of basolateral amygdaloid neurones recorded *in vitro*. *Society for Neuroscience Abstracts* **15**, 193.

WASHBURN, M. S. & MOISES, H. C. (1990). Muscarinic responses of cellular subtypes in rat basolateral amygdala *in vitro*. *Society for Neuroscience Abstracts* **16**, 62.

WILLIAMSON, A. & ALGER, B. E. (1990). Characterization of an early AHP after a brief train of action potentials in rat hippocampal neurons *in vitro*. *Journal of Neurophysiology* **63**, 72–81.

WOMBLE, M. D. & MOISES, H. C. (1990). Voltage-clamp analysis of muscarinic cholinergic actions in rat basolateral amygdaloid neurones recorded *in vitro*. *Society for Neuroscience Abstracts* **16**, 1055.

WOOLF, N. J. & BUTCHER, L. L. (1982). Cholinergic projections to the basolateral amygdala: a combined Evans Blue and acetylcholinesterase analysis. *Brain Research Bulletin* **8**, 751–763.